



Article

Resilience of the Central Indian Forest Ecosystem to Rainfall Variability in the Context of a Changing Climate

Beependra Singh ¹, Chockalingam Jeganathan ^{1,*}, Virendra Singh Rathore ¹, Mukunda Dev Behera ², Chandra Prakash Singh ³, Parth Sarathi Roy ⁴ and Peter M. Atkinson ⁵

¹ Department of Remote Sensing, Birla Institute of Technology (BIT), Mesra, Ranchi 835215, India; phdrs10001.17@bitmesra.ac.in (B.S.); vsrathore@bitmesra.ac.in (V.S.R.)

² Centre for Oceans, Rivers, Atmosphere and Land Sciences (CORAL), Indian Institute of Technology (IIT), Kharagpur 721302, India; mdbehera@coral.iitkgp.ac.in

³ Agriculture and Land Ecosystem Division, Space Applications Centre (SAC), ISRO, Ahmedabad 380015, India; cpsingh@sac.isro.gov.in

⁴ Sustainable Landscapes and Restoration, World Resources Institute India, New Delhi 110016, India; parth.roy@wri.org

⁵ Lancaster Environment Centre, Lancaster University, Bailrigg, Lancaster LA1 4YW, UK; pma@lancaster.ac.uk

* Correspondence: jeganathan@bitmesra.ac.in

Abstract: Understanding the spatio-temporal pattern of natural vegetation helps decoding the responses to climate change and interpretation on forest resilience. Satellite remote sensing based data products, by virtue of their synoptic and repetitive coverage, offer to study the correlation and lag effects of rainfall on forest growth in a relatively longer time scale. We selected central India as the study site. It accommodates tropical natural vegetation of varied forest types such as moist and dry deciduous and evergreen and semi-evergreen forests that largely depend on the southwest monsoon. We used the MODIS derived NDVI and CHIRPS based rainfall datasets from 2001 to 2018 in order to analyze NDVI and rainfall trend by using Sen's slope and standard anomalies. The study observed a decreasing rainfall trend over 41% of the forests, while the rest of the forest area (59%) demonstrated an increase in rainfall. Furthermore, the study estimated drought conditions during 2002, 2004, 2009, 2014 and 2015 for 98.2%, 92.8%, 89.6%, 90.1% and 95.8% of the forest area, respectively; and surplus rainfall during 2003, 2005, 2007, 2011, 2013 and 2016 for 69.5%, 63.9%, 71.97%, 70.35%, 94.79% and 69.86% of the forest area, respectively. Hence, in the extreme dry year (2002), 93% of the forest area showed a negative anomaly, while in the extreme wet year (2013), 89% of forest cover demonstrated a positive anomaly in central India. The long-term vegetation trend analysis revealed that most of the forested area (>80%) has a greening trend in central India. When we considered annual mean NDVI, the greening and browning trends were observed over at 88.65% and 11.35% of the forested area at 250 m resolution and over 93.01% and 6.99% of the area at 5 km resolution. When we considered the peak-growth period mean NDVI, the greening and browning trends were as follows: 81.97% and 18.03% at 250 m and 88.90% and 11.10% at 5 km, respectively. The relative variability in rainfall and vegetation growth at five yearly epochs revealed that the first epoch (2001–2005) was the driest, while the third epoch (2011–2015) was the wettest, corresponding to the lowest vegetation vigour in the first epoch and the highest in the third epoch during the past two decades. The study reaffirms that rainfall is the key climate variable in the tropics regulating the growth of natural vegetation, and the central Indian forests are dominantly resilient to rainfall variation.

Keywords: rainfall; anomalies; NDVI; vegetation; resilient; India; tropical forest



Citation: Singh, B.; Jeganathan, C.; Rathore, V.S.; Behera, M.D.; Singh, C.P.; Roy, P.S.; Atkinson, P.M.

Resilience of the Central Indian Forest Ecosystem to Rainfall Variability in the Context of a Changing Climate. *Remote Sens.* **2021**, *13*, 4474. <https://doi.org/10.3390/rs13214474>

Academic Editor: Brigitte Leblon

Received: 2 September 2021

Accepted: 2 November 2021

Published: 8 November 2021

Publisher's Note: MDPI stays neutral with regard to jurisdictional claims in published maps and institutional affiliations.



Copyright: © 2021 by the authors. Licensee MDPI, Basel, Switzerland. This article is an open access article distributed under the terms and conditions of the Creative Commons Attribution (CC BY) license (<https://creativecommons.org/licenses/by/4.0/>).

1. Introduction

Global warming continues as a consequence of the emission of greenhouse gases (GHG) [1]. Global warming has changed global climatic circulation and has adversely affected the distribution and functioning of natural vegetation [2,3]. In the past few decades,

recurring natural threats such as drought, fire, landslides, floods and anthropogenic threats such as illegal mining, deforestation and agricultural activities worldwide are potential causes of disturbances and changes in the natural vegetation regime [4]. Hansen et al. [5] revealed a forest cover loss of 230 Mha and gain of 80 Mha during 2000–2012 at a global level. Other studies also revealed that global forest cover has decreased from 4128 to 3999 Mha during 1990–2015 [6], and 420 Mha of the global forest area has been lost due to deforestation during 1990–2020 [7]. Such deforestations have a serious effect on rainfall distribution and would alter the structure and functions of the forest [8,9]. Understanding rainfall variation with respect to changes and fluctuations in the forested landscape is important [10,11], as it can be a useful input to models of ecological and environmental processes at local, regional and global scales. Hence, understanding the changing climatic conditions and their association with forest growth patterns is vital for decision makers, planners, the timber industry and ecologists for conservation practices [12,13].

Several studies have been conducted in order to characterize vegetation growth under different climatic conditions. For example, vegetation growth in the higher latitudinal regions or alpine regions is relatively more influenced by accumulated ground/soil temperature than air temperature [14,15] and in the sub-tropical to tropical regions by both solar radiation and water availability [16,17]. In the Amazon, Congo and Indonesia, dense evergreen rainforest growth is driven by solar radiation [18–20]. Moreover, studies have been conducted to characterize the behavior of vegetation growth at different latitudes and its dependency on environmental and climatic factors and factors affecting plant functional traits in tropical species (i.e., inter-annual water uptake, carbon and energy balance) [21,22]. Vegetation dynamics at different altitudes are influenced by moisture availability in the soil and growing season length [23,24].

In the last few decades, remote sensing satellite-based continuous time-series data have become the most reliable means for conducting long-term regional level studies. Satellite data-based vegetation indices, including the Normalized Difference Vegetation Index (NDVI), and climatic parameters have been used to reveal vegetation dynamics and their responses on a monthly, inter-annual basis, capturing any heterogeneity and shifts in biodiversity [25]. NDVI coupled with climatic data has also been used widely for studying climate impacts on vegetation, forest dynamics and vegetation vigour [26–29], as temperature and rainfall are important factors affecting photosynthesis in plants [30]. In recent years, an increase in the number of extreme events (warming and precipitation with different intensity and magnitudes) has been experienced during both summer and winter [31–33]. These have affected the process of vegetation growth, resulting in changes in tropical forest survival strategies.

Chaturvedi et al. [34] modeled the impact of climate change over India and found that the central Indian forests are vulnerable to climate change and need to be further assessed. Nobre et al. [3] observed high evapotranspiration due to increased warming over the central Indian tropical forested regions. Moreover, increased warming and high evapotranspiration can result in changes in micro-climate and energy flux patterns at the regional level [35], including changes in the global climatic pattern and its circulation [36]. However, some studies have reported a decline in rainfall over central India on an annual basis [37,38]. At the same time, an increase in extreme rainfall events has been observed in the last five decades [39–41]. Therefore, it is important to assess the dependence of vegetation on rainfall in the central Indian landscape as changes in rainfall patterns and distribution can alter ecosystem balance, biodiversity and forest productivity. Historically, the vegetation response to changing climate in different years on an inter-annual basis has been complex. The complexity further increases with differences in water and light availability, forest species and local weather conditions prevailing in the region [42,43]. Various studies have analysed the spatio-temporal variability in rainfall to investigate its relationship with different ecophysiological processes that stimulate and enhance plant growth and interactions at a local, regional and global scale [44–47].

The human and natural ecosystem in the central Indian region depends heavily on rain water, and this region receives most of its rainfall during the southwest monsoon, which makes it a climatically vulnerable region in India. The central Indian forest landscape is a vast region and is characterized by an intricate ecosystem with spatially varying vegetation productivity and heterogeneity distributed across different climatic extremes in different seasons. The regional landscape response to gradual climate change has received minimal attention. Hence, it is important to study and understand the spatial variability of rainfall and its effect on vegetation vigour in central India.

Wang et al. [48] studied the response of dry tropical vegetation growth during dry and wet years and found that it varies with temperature and rainfall. As the availability of sunlight in central India is abundant, rainfall deficit does alter and impact the vegetative response and growth patterns, but its spatial variability is still not studied. Therefore, it would be interesting to understand the role of rainfall over the central Indian forested landscape, which provides vital ecosystem services to this region. In this context, this research aims to (i) quantify and understand the variability and trends in spatial rainfall patterns and seasonal vegetation dynamics at annual, short-term and long-term intervals and to (ii) analyze the response of forest to regional rainfall patterns and examine the relationship during different phases.

2. Materials and Methods

2.1. Study Area

The central Indian landscape, a drought-prone region of India, was selected for this study (Figure 1). The study area is extended in five states of India, such as Maharashtra (MH), Madhya Pradesh (MP), Chhattisgarh (CH), Jharkhand (JH) and Odisha (OD). The Bundelkhand, Marathwada and Vidarbha regions of this area have a long history of droughts [49]. The region is rich in flora and fauna with all major forest types (tropical dry and moist deciduous forest, thorn and scrub forest, tropical evergreen and semi-evergreen forest). Sal, teak and bamboo are the main vegetation species [50]. The human population of the area is largely dependent on the forests for its livelihood. The region has complex ecosystems consisting of several hill ranges (Vindhyan Range, Satpura Range, Chhota Nagpur Plateau, Deccan Plateau, Western Ghats and the Eastern Ghats), river systems (Tapi, Narmada, Godavari, Krishna and Mahanadi) and forests.

The study area is adjacent to the alluvial plain of the Ganga river in the north, the Thar desert in the north–west, the Bay of Bengal in the south–east, the Arabian Sea in the west and the peninsular landscape in the south. The area's geographical extent is approximately 9,86,580 km² of which 2,61,120 km² (26.46%) is under forest [51]. The climate of the region is mostly warm, with very high temperatures during the summer. It experiences a minimum temperature of 5 degrees Celsius during the winter season (November–February) and a maximum temperature of 45 degrees Celsius during the summer (March–June). It receives the majority of its rainfall from the southwest monsoon.

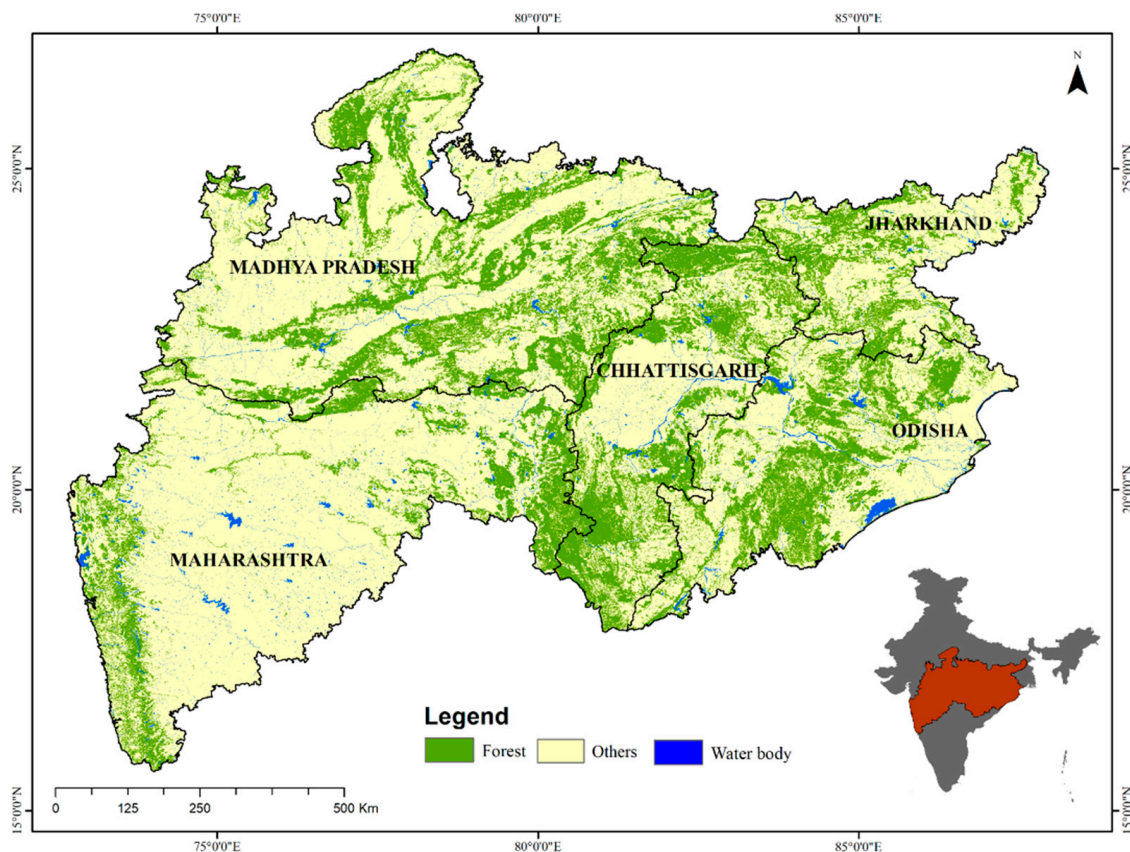


Figure 1. Study area.

2.2. Data

This research used the precipitation data of the Climate Hazards Group Infra-Red Precipitation with Station dataset (CHIRPS version 2.0), with CHIRPS being the longest archived global precipitation dataset. The data are available from 1981 onwards for latitudes 50°S – 50°N and all longitudes at a spatial resolution of 0.05° (~ 5 km). These have been used extensively for rainfall trend analysis and drought monitoring. For this research, 18 years (2001 to 2018) of monthly precipitation data were downloaded from the site (<ftp://ftp.chg.ucsb.edu/pub/org/chg/products/CHIRP/monthly/>, Accessed on 2 July 2018) [52]. Moreover, 18 years of NDVI time-series data from the Moderate Resolution Imaging Spectro-radiometer (MODIS), specifically MOD13Q1 V6 Terra composites of 16-day interval at 250 m spatial resolution, were downloaded from the Land Processing Distributed Active Archive Center (LPDAAC) (<https://lpdaac.usgs.gov/>, Accessed on 11 January 2019). The MODIS standard VI products time-series data are atmospherically corrected for bi-directional surface reflectance and are usually masked for water, clouds, heavy aerosols and cloud shadows before archiving for end users [53,54]. Moreover, we used the most recent comprehensive vegetation type map (<http://bis.iirs.gov.in/>, Accessed on 20 January 2019) produced at 1:50,000 scale using the LISS III sensor (23.5 m) for the Indian subcontinent by Roy et al. [55] to generate the forest mask at 5 km spatial resolution.

2.3. Methods

MODIS tiles (6 tiles, i.e., h24v06, h24v07, h25v06, h25v07, h26v06 and h26v07) consisting of a total of 2,484 images (23 tiles per year for 18 years) were analyzed. Only pixels with pixels reliability values of 0 (good data) and 1 (marginal data) were considered for further analysis, while the rest of the pixels were discarded. Then, year-wise, tiles were mosaicked. The NDVI data gaps due to clouds were filled with noise-free temporal neighborhood values without compromising the annual growth profile of natural vegetation. Erroneous

values in the derived annual stacked images at each pixel level were eliminated by applying the statistical outlier removal technique. Finally, noise-free data were smoothed by using Discrete Fourier Transform (DFT) [56–58]. The smoothed NDVI data were upscaled from 250 m to 0.05° (~ 5 km) by using mean aggregation to match the spatial resolution of the rainfall data. To strengthen the analysis, we considered only the forested pixels based on a forest mask at 5 km (see Singh et al. [29] for further details). A methodology representing the entire procedure involved in this study is shown in Figure 2.

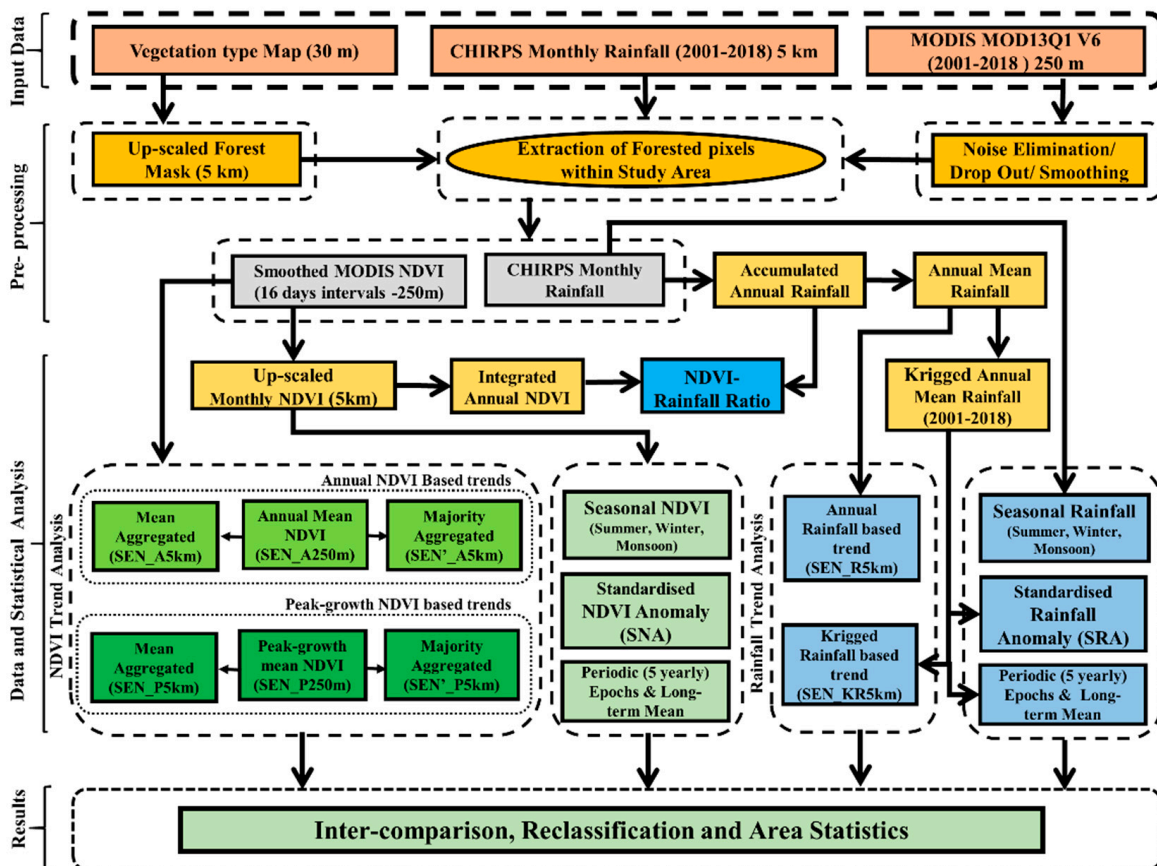


Figure 2. The overall methodology.

2.3.1. Trend Analysis and Statistical Significance

In this research, a trend analysis of 18 years of rainfall and NDVI data was undertaken to determine their variability over time. Such trend analysis is very common and helpful in climate science, hydrology and vegetation dynamics [25]. Among the available methods, the Mann–Kendall test and Sen’s slope are commonly used to estimate the upward or downward trend of the time-series. However, Sen’s slope test is the most common method for estimating the magnitude of and understanding the significance of any trend in the time-series data [25,59–62]. While performing trend analysis, we observed noise in the resultant map as vertical stripes and linear patches. In order to avoid such errors, we converted all the input rainfall data into points and interpolated using Ordinary Kriging, which helped to remove the outliers in the input rainfall data. The trend results from interpolated and original rainfall data were compared for their reliability (see Supplementary Figure S1), and Krigged results could remove the stripping noise and correctly preserved the spatial and temporal variations. The results obtained from the long-term trend analysis were used to characterize the increasing and decreasing trends in rainfall data and the NDVI data to quantify any greening and browning pattern in the Central Indian forested landscape.

2.3.2. Rainfall and NDVI Anomalies

The impact of rainfall variability on vegetation in the Central Indian landscape was characterized based on analysis of time-series anomalies. The response of vegetation to moisture availability was analysed specifically in dry, normal and wet years. The spatio-temporal variability in rainfall anomalies was produced using the annual mean rainfall from 2001 to 2018. Equation (1) is the standard anomaly equation generally used in statistics to estimate the Z-score [63]. Since the study covers a vast region from the western coast to the eastern coast of India, rainfall quantity is different in dry and wet regions. Thus, we have to standardize rainfall in order to compare the relative intra and inter-annual variability over the study region:

$$\text{SRA}(i, x, y) = \frac{\text{Rainfall}(i, x, y) - \text{Mean}[\text{Rainfall}_{2001-2018}(i, x, y)]}{\text{STD}[\text{Rainfall}_{2001-2018}(i, x, y)]} \quad (1)$$

$$\text{SNA}(i, x, y) = \frac{\text{NDVI}(i, x, y) - \text{Mean}[\text{NDVI}_{2001-2018}(i, x, y)]}{\text{STD}[\text{NDVI}_{2001-2018}(i, x, y)]} \quad (2)$$

where $\text{SRA}(i, x, y)$ represents the annual standardized rainfall anomaly (SRA) in the i th year at the pixel location (x, y) and $\text{rainfall}(i, x, y)$ represents the annual rainfall of i th year being processed. $\text{Mean}[\text{rainfall}_{2001-2018}(i, x, y)]$ represents the long-term mean annual rainfall from 2001 to 2018. $\text{STD}[\text{rainfall}_{2001-2018}(i, x, y)]$ represents the standard deviation of annual rainfall from 2001 to 2018. Moreover, we computed the annual standardized NDVI anomaly (SNA) for 18 years by using Equation (2) with the same approach as mentioned above for Equation (1). Here, the negative SRA values in a year correspond to less rainfall than the average, while positive SRA values indicate surplus rainfall. Similarly, the negative SNA values indicate stress or degradation or deforestation. On the other hand, positive SNA implies increased vegetation vigour (greening).

2.3.3. Seasonal and Periodic Variability in the Vegetation and Rainfall

We evaluated the long-term seasonal variability of rainfall and NDVI over 18 years. First, we derived the three different seasonal means from monthly rainfall: summer (March, April and May), monsoon (June, July, August, September and October) and winter (November, December, January and February). However, on the other hand, NDVI composites of 16 days intervals with a spatial resolution of 250 m were temporally averaged into a monthly composite. These monthly composites were spatially upscaled from 250 m to 5 km monthly NDVI by using the mean aggregation method to match rainfall resolutions. Then, NDVI monthly data were converted into three seasonal data as mentioned above. Finally, the long-term mean NDVI and rainfall in these three seasons were estimated and compared in order to understand the seasonal variability and dependency effect of rainfall on vegetation. Moreover, we explored the forest–rainfall feedback over different epochs (first epoch—2001 to 2005; second epoch—2006 to 2010; third epoch—2011 to 2015; fourth epoch—2016 to 2018). Similarities in the difference pattern of rainfall and NDVI between these epochs were checked in different phases for understanding the responses of vegetation to rainfall (i.e., 1st phase = second epoch – first epoch; 2nd phase = third epoch – second epoch; 3rd phase = fourth epoch – third epoch). The annual rainfall maps using ordinary kriging was used instead of the original CHIRPS data.

2.3.4. NDVI-Rainfall Ratio

The photosynthetic productivity of an ecosystem in a region is related directly to the total water use for carbon assimilation per unit of soil water loss [64], especially in tropical climates. In this regard, we estimated the spatial distribution of proxy water use efficiency based on the ratio of yearly integrated NDVI and accumulated rainfall,

as both are correlated [65,66]. The potential water use efficiency was estimated by the NDVI-Rainfall Ratio (NRR) in this study (Equation (3)):

$$\text{NDVI_Rainfall Ratio(NRR)}_i = \frac{\sum_{c=1}^N \text{NDVI}_c}{\sum_{d=1}^M RF_d} \quad (3)$$

where c , d refers to composite number, N is the total number of NDVI composites and M is the total number of rainfall composites in i th year.

2.3.5. Sensitivity to Spatial Resolution, Growth Period and Aggregation Method

Furthermore, we analysed the consistency in Sen's slope for long-term trends with respect to (a) different spatial resolutions (250 m and 5 km), (b) different temporal growth periods and (c) different aggregation methods. First, we considered the smoothed NDVI data at 250 m resolution and then estimated mean NDVI over the entire annual cycle (NDVI-A250) and mean NDVI during the peak growth period (NDVI-P250). Generally, peak growth period refers to the period where NDVI values are greater than 50% of the maximum annual NDVI (see Singh et al. [29] and Rajan and Jeganathan [67] for details). In central India, the major vegetation vigour is observed during July, August, September and October. Hence, in this research, we estimated the mean NDVI during these periods, referred to as NDVI_P250. Using these two datasets, we estimated Sen's slope. Similarly, Sen's slope was estimated for the mean aggregated 5 km NDVI from annual and peak periods (NDVI-A5km and NDVI-P5km). These four Sen's slope datasets (SEN-A250, SEN-P250, SEN-A5km and SEN-P5km) were reclassified into ten classes, and the consistency in their area statistics was analyzed. Finally, the 250 m trend datasets were aggregated to 5 km for which we followed a 2-tier approach where first, the Sen's slope images were reclassified, and then the majority slope class within the 5 km grid was chosen. Importantly, converting Sen's slope values directly from 250 m to 5 km based on the majority function would be error prone. The majority based aggregation function is reliable only on nominal data and not on continuous data where variation may be greater. Hence, 250 m trend values (SEN-A250 and SEN-P250) were first reclassified into 10 classes and then aggregated to 5 km based on the majority class (referred as SEN'_A5km, SEN'_P5km). These six outcomes were analyzed for their consistency based on area statistics.

3. Results

3.1. Long-Term Trend Analysis of Rainfall and Vegetation

Figure 3a reveals the long-term mean rainfall, and Figure 3d reveals the long-term mean NDVI for the period 2001 to 2018. The results show that the long-term mean rainfall was low in the north-west direction of the study area and high in the Western Ghats and eastern region.

The long-term mean NDVI exhibited a clear correlation with rainfall with a larger mean NDVI in the east of the study area and the Western Ghats. In contrast, the western part of MP exhibited smaller mean values of NDVI where rainfall was low. The long-term rainfall (Figure 3b) and NDVI (Figure 3e) trends were estimated by using Sen's slope analysis at the pixel level, which revealed an interesting pattern of decreasing and increasing trends in different areas across the landscape (Figure 3b). The largest increasing trend was seen in the western part of MP, JH and the Western Ghats, covering an area of 0.3% (1100 km²). Increasing rainfall trends, grouped into positive Sen's slope classes of 0–0.5, 0.5–1 and 1–1.5 were observed over 30.36%, 21.92% and 6.38% of the area. The Western Ghats, MH, south-eastern parts of MP, southern parts of CH, the central part of OD and the north-eastern region of JH showed a decreasing rainfall trend grouped into negative Sen's slope classes of –1.4 to –1, –1 to –0.5 and –0.5 to 0, covering 2.18%, 11.16% and 27.72% of the area, respectively. A positive NDVI trend was distributed spatially over much of the study region, and the classes >0.002 and 0.001–0.002 revealed the locations of increasing NDVI over 56.77% and 26.29% of the area, respectively. The negative NDVI

trend classes of < -0.003 , -0.003 to -0.002 and -0.002 to -0.001 are mainly confined to small parts of the northern region, being observed over 0.15%, 0.08% and 0.43% of the area, respectively. Significant pixels of increasing and decreasing trends as shown in Figure 3c,f were validated for their reliable increasing and decreasing trend for Rainfall and NDVI (see Figure S2). Figure 4 reveals the representative vegetation growth pattern of evergreen, semi-evergreen, moisture and dry deciduous vegetation types for 18 years (2001 to 2018).

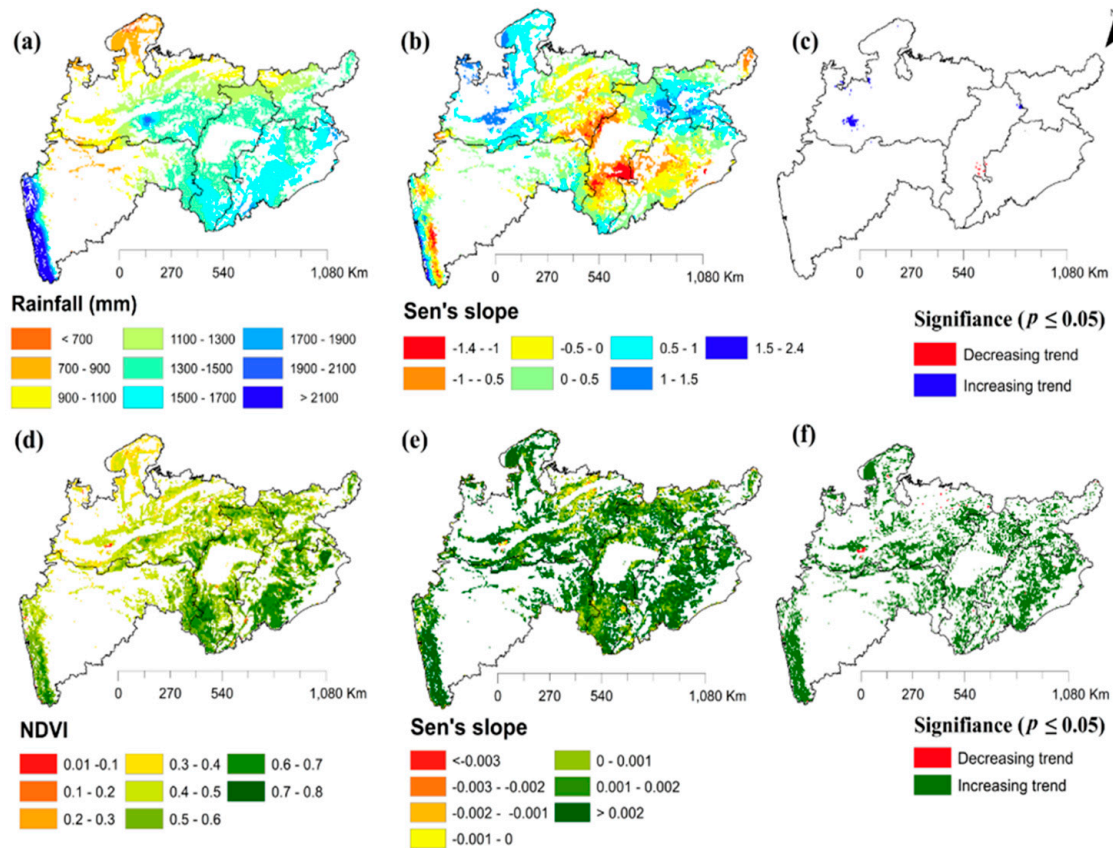


Figure 3. (a,d) Spatial distribution of long-term mean, (b,e) Sen's Slope and (c,f) significance from 18 years (2001–2018) of (a–c) rainfall and (d–f) NDVI datasets.

3.2. Inter-Annual Variability of Rainfall Anomaly

The Standardised Rainfall Anomaly (SRA) reveals any statistical variability in rainfall, with different categories of anomaly depicting different levels of water stress (i.e., negative anomaly) or wetness (i.e., positive anomaly) in different years (Figure 5). Table 1 shows the percentage area under different negative and positive anomalies in dry, normal and wet years. The central Indian forest experienced extreme drought conditions during 2002 (98.24% of the area), 2004 (92.81% of the area), 2009 (89.55% of the area), 2014 (90.11% of the area) and 2015 (95.80% of the area). However, surplus rainfall was observed in 2003 (69.52%), 2005 (63.93%), 2007 (71.97%), 2011 (70.35%), 2013 (94.79%) and 2016 (69.86%). Among these years, 2002 was the most extreme dry year, and 2013 was the wettest year. During 2001–2018, on average, 46.52% of the area experienced positive anomalies. While 53.48% area showed negative anomalies, of which 15.38% of the area suffered from dry conditions (i.e., < -1 SRA) and 16.61% of the area from wet condition (excess rainfall, i.e., > 1 SRA) (see Supplementary Table S1 for more details on percentage area under different negative and positive anomalies from 2001 to 2018).

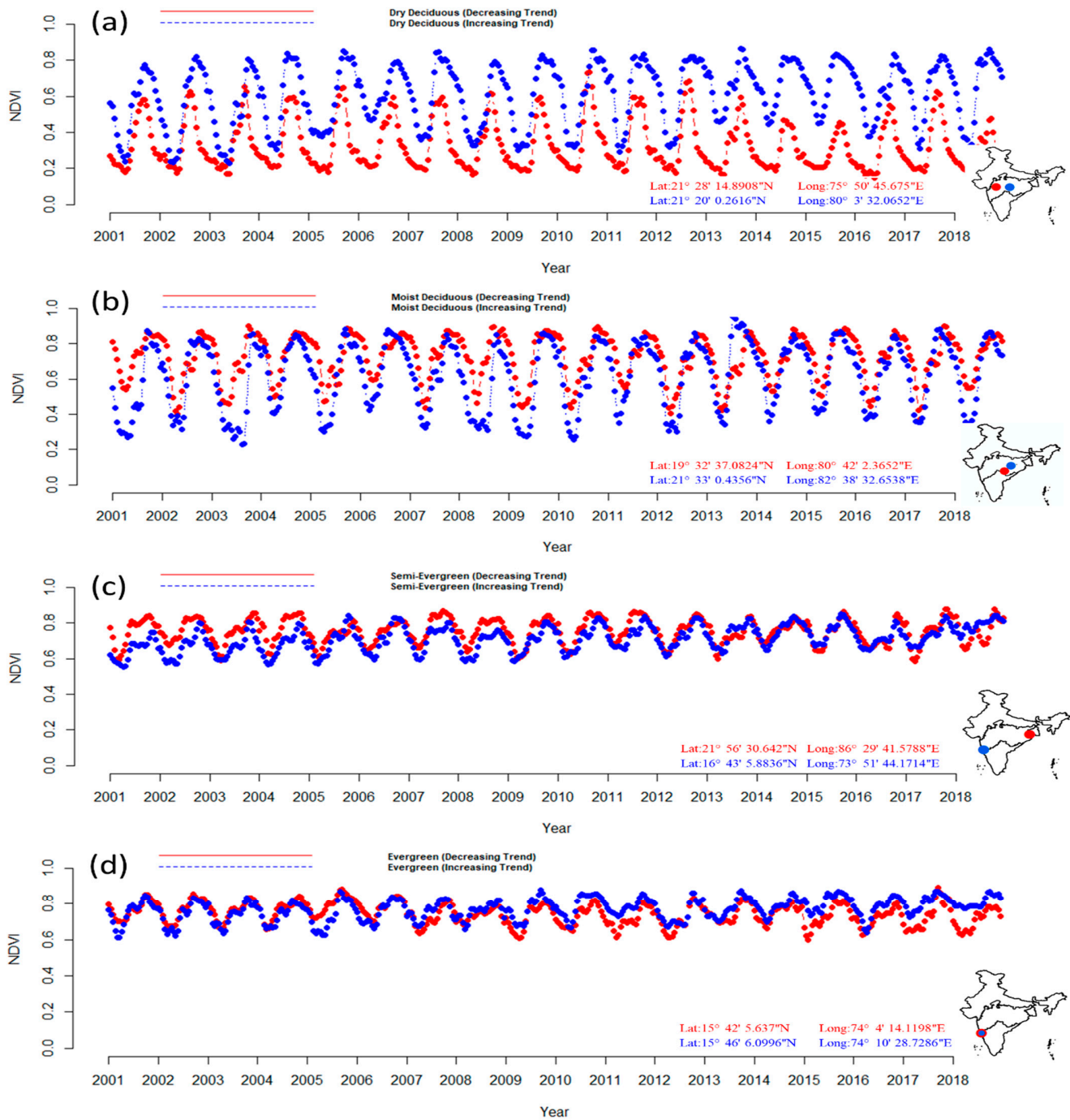


Figure 4. Time series vegetation growth profile from 2001 to 2018 for four vegetation types: (a) dry deciduous, (b) moist deciduous, (c) semi-evergreen and (d) evergreen (note: the decreasing trend and increasing trend in NDVI area are shown in red and blue color, respectively).

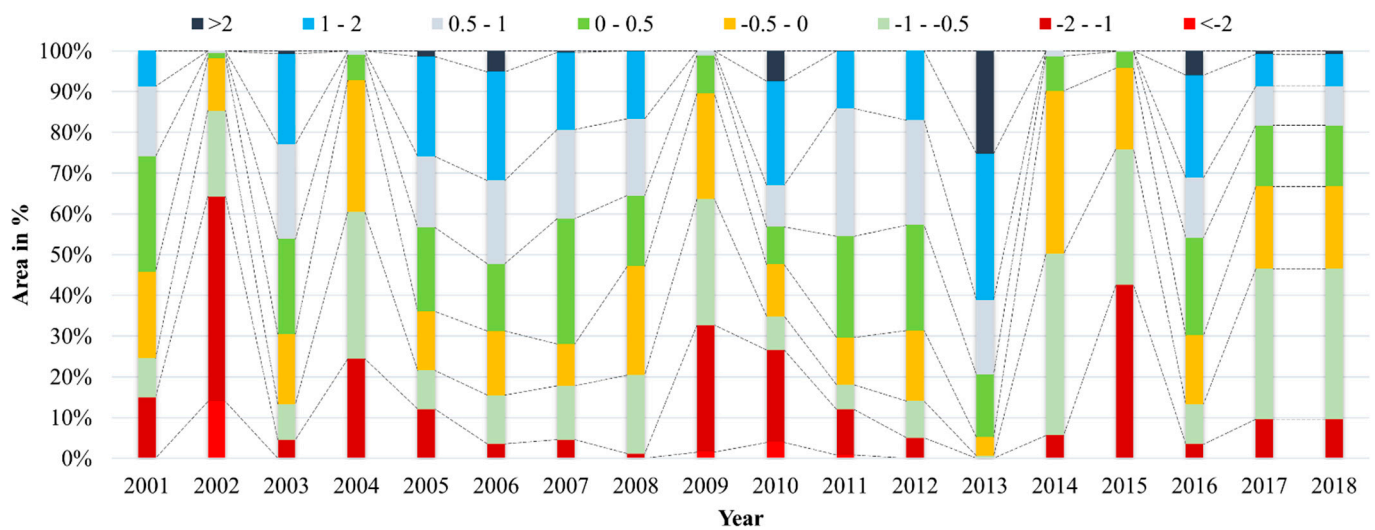


Figure 5. Standardized rainfall anomaly (SRA) over 18 years (2001–2018).

Table 1. Standardised Rainfall Anomaly (SRA) during dry, normal and wet years.

SRA	Anomaly Classes	2002	2011	2013
<−2	Extremely Dry	13.99	0.84	0
−2−−1	Very Dry	50.3	11.21	0.01
−1−−0.5	Moderately Dry	21.05	6.02	0.61
−0.5−0	Normal	12.9	11.58	4.59
0−0.5	Normal	1.25	24.89	15.35
0.5−1	Moderately Wet	0.52	31.33	18.29
1−2	Very Wet	0	14.08	35.93
>2	Extremely Wet	0	0.05	25.23

3.3. Vegetation Response to Seasonal Rainfall Variation

Figure 6 shows the spatial distribution of the season-wise (i.e., winter, summer and monsoon) long-term mean rainfall and NDVI from 2001 to 2018. Although rainfall varied drastically with the seasons in central India, the large NDVI values in all three seasons indicate the presence of a great expanse of natural vegetation in the study area, with evergreen/semi-evergreen in the western and seasonal rainfall-dependent deciduous vegetation in the remaining part. During the winter (Figure 6a), the central and southeastern regions received a certain amount of rainfall (up to 30 mm), while the western part received scant rainfall. However, a moderate increase in rainfall intensity was observed with the arrival of summer (Figure 6b), with less rainfall amount in the western regions. Interestingly, the high-density forest in the eastern parts of Odisha (OD), Jharkhand (JH) and Chhattisgarh (CH) received a higher amount of rainfall in the summer. However, during the monsoon, the Western Ghats and western regions received the highest rainfall, the central and eastern regions received moderate-to-high rainfall and the north-western region had the least rainfall (Figure 6c).

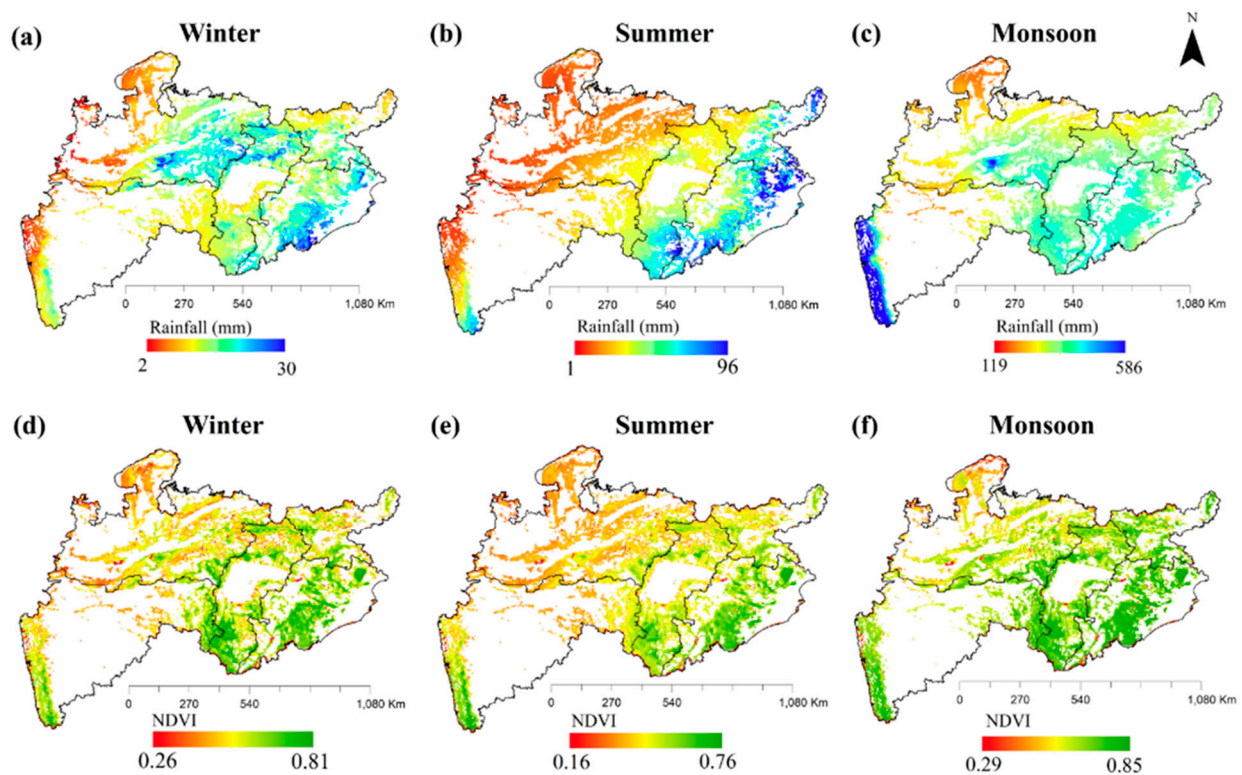


Figure 6. Spatial distribution of long-term (2001–2018) in (a–c) mean seasonal rainfall and (d–f) mean seasonal NDVI.

We also analyzed the seasonal mean NDVI and its response to rainfall variability for the same period. During the winter, the regions with the most rainfall (i.e., the eastern region and parts of WG) showed a healthy vegetation condition where evergreen/semi-evergreen/moist-deciduous vegetation is dominant (Figure 6d). Nevertheless, during the summer season, due to heatwaves, browning of vegetation was observed over the vast stretches of the central and north-western regions of the study area where dry deciduous vegetation is dominant (Figure 6e). The seasonal NDVI variability revealed the phenological cycle in central India. The natural vegetation here attains peak growth with maximum greenness during the monsoon and senescence during the dry conditions in summer and winter. Its spatial variability is linked with species types (Figure 6d–f).

3.4. Periodic (5 Yearly) Rainfall and Vegetation Sensitivity

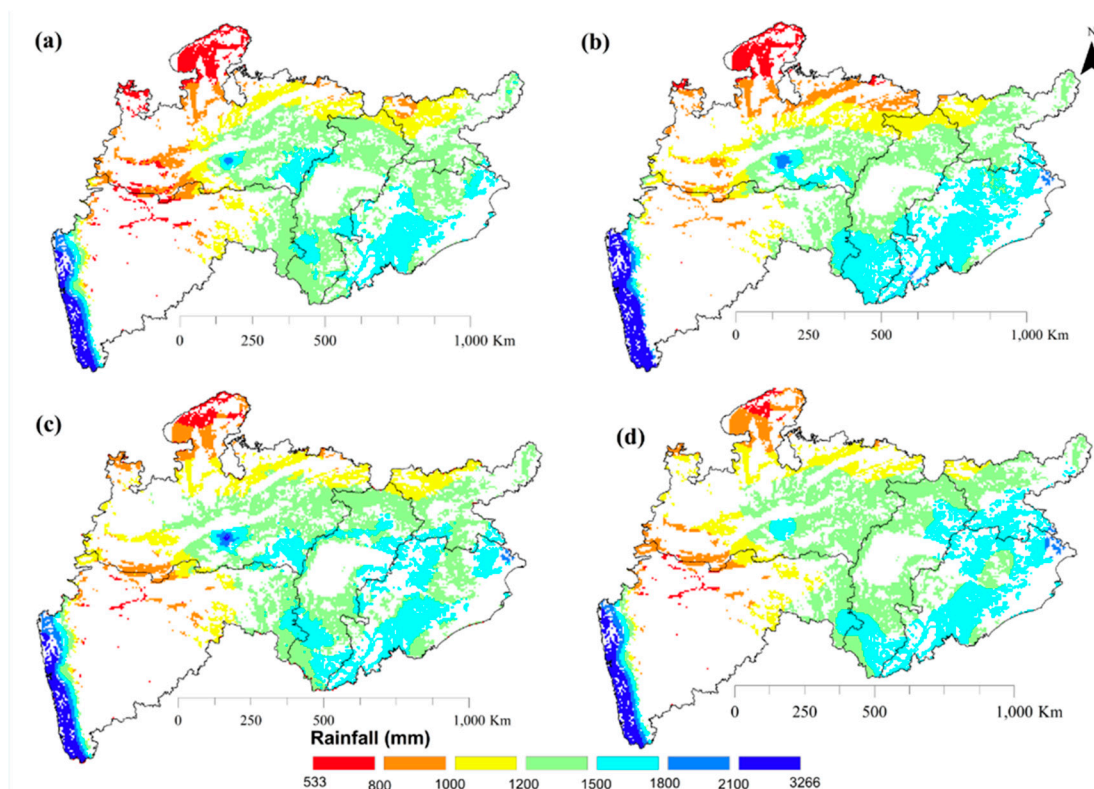
The entire study period was divided into four epochs (i.e., 2001–2005, 2006–2010, 2011–2015 and 2016–2018) so that the annual rainfall and NDVI variability can be better characterized in different epochs, as shown in Tables 2 and 3. The spatial pattern of mean annual rainfall was more-or-less consistent in different epochs with minor variability, which can be observed in Figure 7a–d. The annual rainfall has increased over the years, which can be observed through the increasing areal coverage of the 1200–1500 mm class and a relative decrease in the <800 mm class area in Table 3. This may have contributed to vegetation growth, as observed by the increase in the area of the NDVI class >0.6 in different epochs. The first epoch (2001–2005) was a relatively drier period than the other epochs. In all the epochs, the Western Ghats region consistently received the maximum rainfall due to its topographic alignment, and the north-western part of MP received the lowest rainfall.

Table 2. Percentage area distribution of rainfall in different epochs.

Rainfall (mm)	Epoch 1 2001–2005	Epoch 2 2006–2010	Epoch 3 2011–2015	Epoch 4 2016–2018
<800	7.31	4.84	2.23	1.78
800–1000	8.65	9.40	6.86	7.74
1000–1200	15.55	16.63	15.34	13.53
1200–1500	47.22	36.26	46.62	47.03
1500–1800	19.22	30.90	26.65	27.75
>1800	2.05	1.97	2.30	2.18

Table 3. Percentage area distribution of NDVI in different epochs.

NDVI	Epoch 1 2001–2005	Epoch 2 2006–2010	Epoch 3 2011–2015	Epoch 4 2016–2018
<0.15	0.31	0.26	0.22	0.08
0.15–0.30	1.24	0.74	0.40	0.41
0.30–0.40	13.35	9.31	6.21	7.42
0.40–0.50	35.12	36.63	33.37	33.41
0.50–0.60	32.47	33.15	33.72	33.46
0.60–0.70	15.66	17.51	21.80	21.29
>0.70	1.85	2.40	4.28	3.93

**Figure 7.** Spatio-temporal variability in the long-term mean annual rainfall in different epochs: (a) 1st epoch (2001–2005), (b) 2nd epoch (2006–2010), (c) 3rd epoch (2011–2015) and (d) 4th epoch (2016–2018).

All epochs experienced three major patterns: high rainfall in the Western Ghats and coastal region, moderate rainfall in the north-eastern region and the lowest rainfall in the north-western region. Interestingly, the mean NDVI in different epochs revealed a consistent pattern of vigour in the classes 0.40–0.50 and 0.50–0.60 (Table 3), which may be

an indication of the strong resilience of the vegetation system in the region. In the first epoch (the driest period in 18 years), the mean NDVI values were consistently smaller in the larger part of the north-western region (Figure 8a), which is a clear indication of the adaptation of vegetation systems in low-rainfall areas.

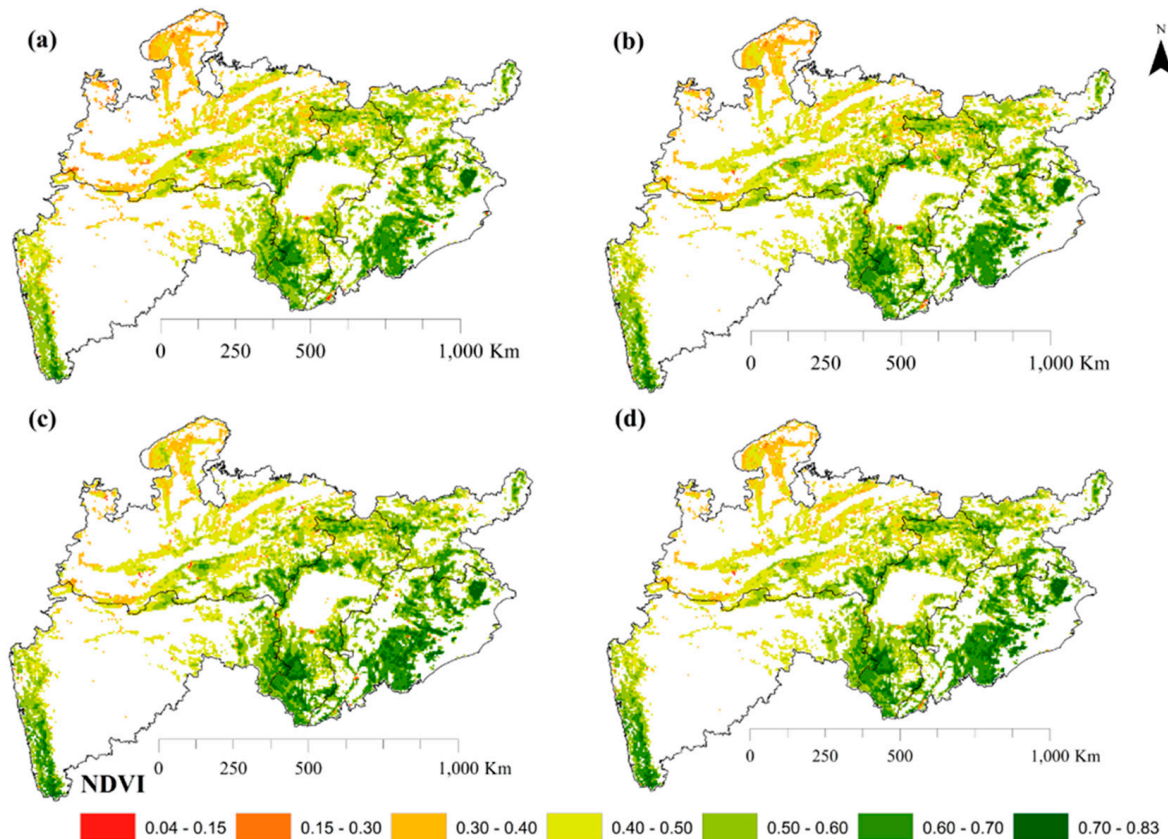


Figure 8. Spatio-temporal variability in the long-term mean annual NDVI in different epochs: (a) 1st epoch (2001–2005), (b) 2nd epoch (2006–2010), (c) 3rd epoch (2011–2015) and (d) 4th epoch (2016–2018).

In fact, these areas are drier regions with scrubs, grasses and thorn vegetation types [68–70] and especially *lantana camara*, which have covered most parts of the protected forests of central India [68,71]. Apart from this, the region is abundant with teak forests [69,72] with low biomass accumulation, which is limited due to environmental conditions compared to other moist forests. The regions with large mean NDVI (class 0.6–0.83) are characterized with densely vegetated areas of moist deciduous forest in the eastern region and evergreen forests in the Western Ghats (Figure 8).

We analyzed the temporal differences in rainfall across different epochs by classifying the derived difference into seven classes (Figure 9a–c). We checked their association with the relative temporal difference in NDVI (Figure 9d–f). Tables 4 and 5 show the area percentage of different classes in three different phases. Here, the difference between epochs is referred to as phases: phase-1 refers to (epoch2-epoch1); phase-2 is (epoch3-epoch2); and phase-3 is (epoch4-epoch3). In phase-1, negative values mean that the current epoch (second) received less rainfall than the previous (first) epoch, and positive values mean that the region received higher rainfall in the current epoch. The phase-1 result (Figure 9a) revealed that in the northern part of the study area (shown in red-to-yellow colour in Figure 9a), the second epoch (2006–2010) received less rain than the first epoch (2001–2005). Interestingly, a similar pattern was observed in NDVI difference, i.e., a decline in vegetation growth in phase-1 revealing a possible regional rainfall dependency (Figure 9a,d). The phase-2 results revealed that the third epoch’s rainfall was greater than the second in the

northern part (Figure 9b). In contrast to the first phase, the spatial pattern of positive NDVI classes showed a gain in vegetation growth and the effect of rainfall in central India (Figure 9e).

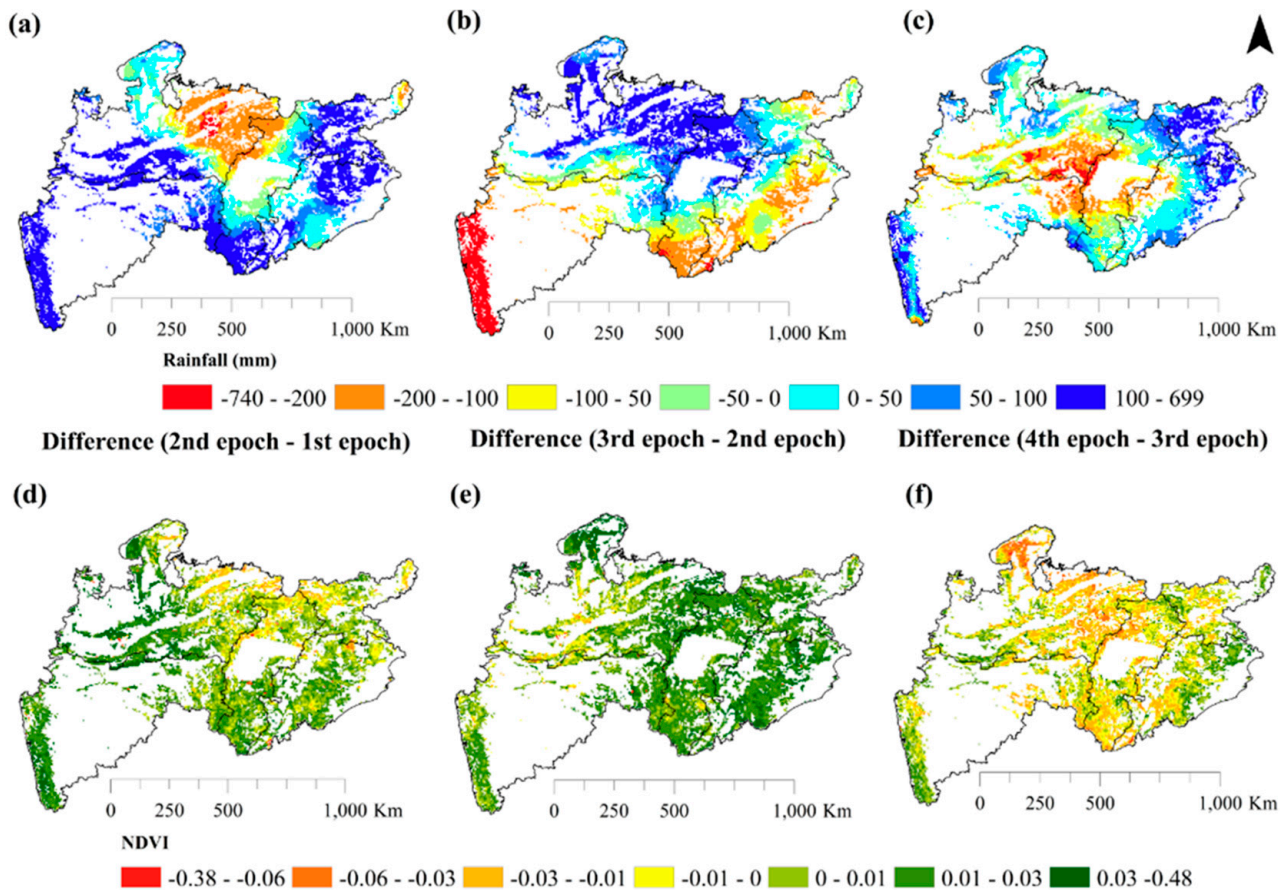


Figure 9. Spatial distribution of 5 yearly differences in (a–c) rainfall and (d–f) NDVI.

Table 4. Percentage area distribution of rainfall difference in different phases.

Rainfall (mm)	Phase 1 (2nd–1st Epoch)	Phase 2 (3rd–2nd Epoch)	Phase 3 (4th–3rd Epoch)
−740−−200	1.06	8.26	2.37
−200−−100	13.87	12.47	14.43
−100−−50	4.03	16.44	12.66
−50−0	7.39	13.07	17.28
0−50	14.48	9.92	21.49
50−100	12.97	13.40	18.93
100−699	46.20	26.44	12.84

In the third phase (Figure 9c), rainfall decline was relatively high, which negatively affected the spatial pattern of vegetation growth in the fourth epoch (Figure 9f). All phases depicted three different patterns: (a) dry spell over the northern region during the first phase, (b) wet spell during the second phase in the north and dry spell in the south and (c) dry spell during the third phase. Overall, there exists a similarity in the spatial pattern between rainfall and NDVI variation, confirming the water dependency of the central Indian vegetation ecosystem in all phases. However, the dependency seems to be much higher in the northern regions than in the south-east. Despite the decline in rainfall in phase 2 (Figure 9b), there was a positive vegetation growth (larger NDVI values in Figure 9e).

Table 5. Percentage area distribution of NDVI difference in different phases.

NDVI	Phase 1 (2nd–1st Epoch)	Phase 2 (3rd–2nd Epoch)	Phase 3 (4th–3rd Epoch)
−0.38–−0.06	0.47	0.27	0.29
−0.06–−0.03	0.31	0.16	3.69
−0.03–−0.01	4.86	1.32	26.77
−0.01–0	14.11	5.38	30.49
0–−0.01	28.45	15.93	24.36
0.01–0.03	41.20	59.97	13.29
0.03–0.48	10.60	16.97	1.11

3.5. Response of Vegetation Growth during Drought, Normal and Wet Years

From the perspective of local and global climate change, it is pertinent to examine the effect of different climatic extremes (dry, wet and normal) on the growth dynamics of natural vegetation. The classified standardized rainfall anomaly (SRA) and Standardised NDVI Anomaly (SNA) maps from 2002 (dry), 2011 (normal) and 2013 (wet) are presented in Figure 10. Around 98.24% of the study area showed a negative rainfall anomaly in 2002 (Figure 10a). There was an apparent reduction in NDVI throughout the study area in 2002, and a positive NDVI anomaly was observed only in 7.09% of the forested area (Figure 9d). During the normal year (2011), around 69.90% of the area observed a positive rainfall anomaly, except in the southern part of CH and OD (Figure 10b). Surprisingly, even in the regions of positive rainfall anomaly in the same year, around 38.51% of the area experienced a negative NDVI anomaly over northern CH and the northwest of OD (Figure 10e).

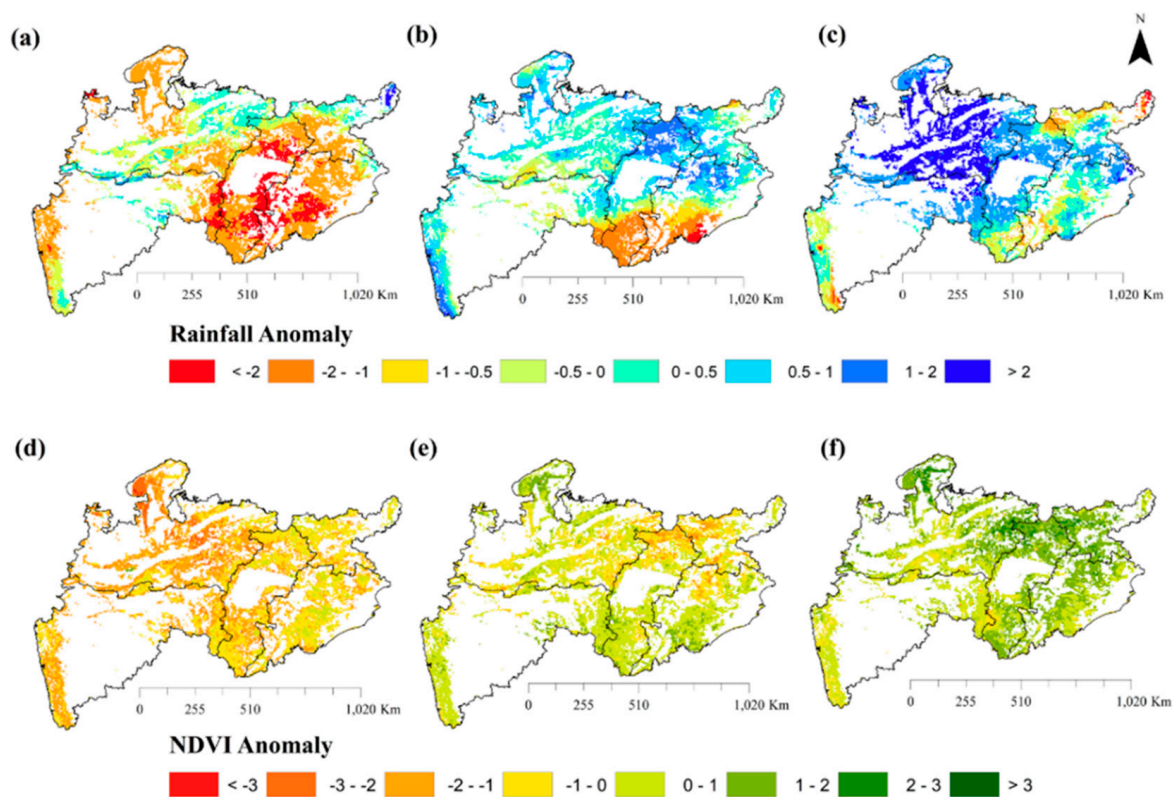


Figure 10. Spatio-temporal variability of rainfall anomaly (a–c) and NDVI anomaly (d–f) in different years: (a,d) dry year (2002), (b,e) normal year (2011) and (c,f) wet year (2013).

In 2013 (wet year), around 94.98% of the area experienced a positive rainfall anomaly except for a few parts of JH, southern OD, CH and the Western Ghats (Figure 10c). In the same year, most vegetation showed a positive growth anomaly (NDVI vigour) over 88.57% of the area (northern and eastern MP, northern CH, most parts of JH and OD), while only 11.43% of the area (southern MP, CH and south-eastern parts of OD) experienced a mild negative anomaly (Figure 10f). However, some regions experienced contrasting positive and negative NDVI anomalies, which might be due to the varying levels of rainfall in the catchments, sub-surface flow, soil moisture, evapotranspiration, water table fluctuation and topographic conditions. Hence, future research is needed to investigate the response of different types of vegetation in different catchments.

3.6. Spatio-temporal Distribution of NDVI-Rainfall Ratio (NRR)

Figure 11d reveals the spatial distribution of long-term mean water use efficiency (i.e., NRR for the study area). It is observed that the average NRR was highest in the south and north and lowest in the Western Ghats, parts of Maharashtra and parts of MP. The variability in NRR is due to the spatial distribution of vegetation type, vegetation adaptation capacity, soil conditions, altitude and runoff. The area of different NRR classes in different climatically extreme years is provided in Table 6.

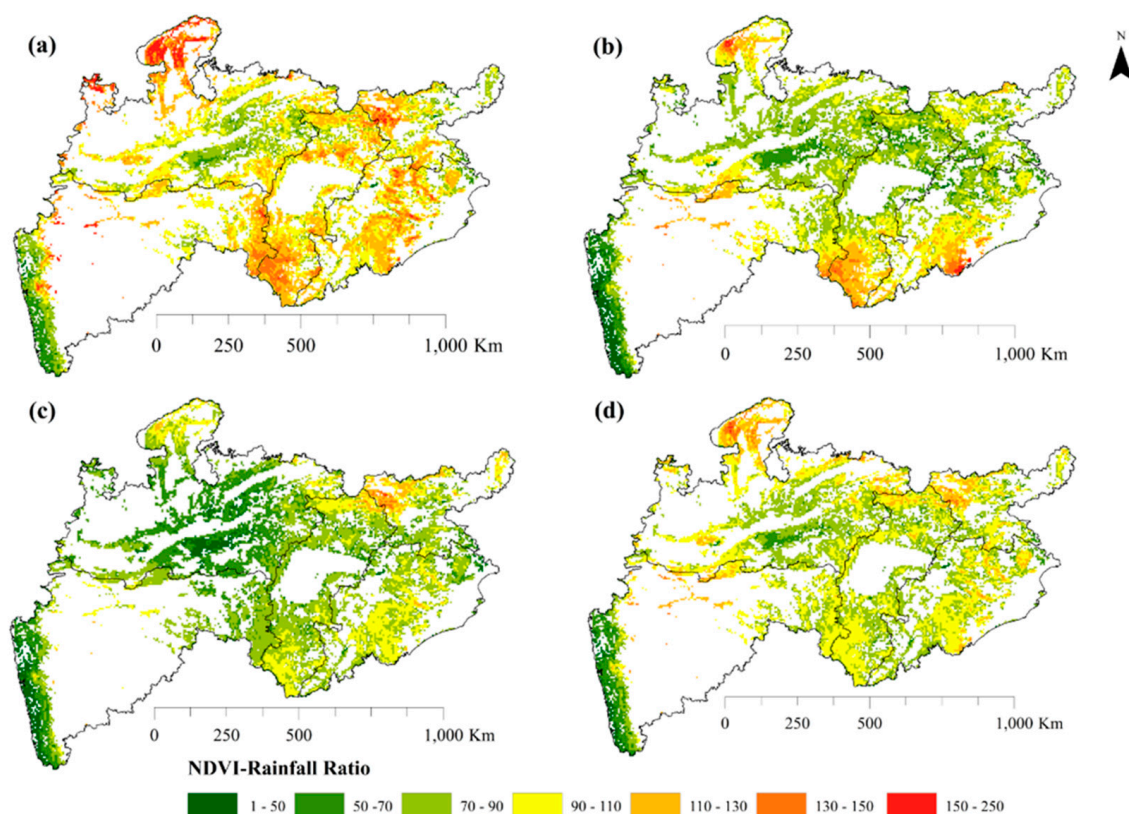


Figure 11. Spatio-temporal variability in the NDVI-Rainfall Ratio (unit mm^{-1}): (a) dry year (2002), (b) normal year (2011), (c) wet year (2013) and (d) long-term mean NDVI-Rainfall Ratio.

Table 6. NRR distribution (in % area) in a dry, normal and wet year and its long-term mean.

NRR Class	Dry Year (2002)	Normal Year (2011)	Wet Year (2013)	Long-Term Mean
1–50	0.65	4.06	6.31	1.81
50–70	5.05	14.98	28.85	8.24
70–90	20.08	42.10	43.64	40.65
90–110	35.90	26.39	18.33	39.60
110–130	27.68	10.23	2.56	8.66
130–150	8.21	1.97	0.30	1.00
150–250	2.43	0.27	0.01	0.04

The long-term mean NRR shows that around 46% of the forested regions had good-to-high NRR, which increased to 74% in the dry year and reduced to 21% in the wet year. NRR can, thus, help in understanding the resilience of the central Indian forest ecosystem as high values of NRR indicate greater adaptability to water stress conditions. In Figure 11d, different values of NRR could be related to different vegetation types such as the dark green colour being related to evergreen forest, yellowish shades are related to semi-evergreen and moist deciduous forest and the red shades for the dry deciduous area.

4. Discussion

The study of terrestrial vegetation and its dynamics is important not only at the regional level but also to help in understanding the impacts of climate change and extreme events on the global scale. This research investigated the spatial pattern of rainfall, its variability and its influence on forests at the regional level in India. In general, the study area experienced entropic rainfall distributions with variation over 18 years. Significant increasing trends in rainfall in MP and decreasing trends in CH were found in this study. Similar decreasing trends were reported by Paul et al. [73]. However, few previous studies have reported an increasing trend in rainfall over central India across different time frames [74,75]. Despite the decreasing rainfall trends, the major proportion of the area showed greening over central India, which might be due to government initiatives related to water conservation measures, afforestation and declines in the rate of deforestation, as revealed by Reddy et al. [76]. Apart from this, aerosol loading in the atmosphere has increased over India [77,78], which, in turn, has helped cloud formation and increased rainfall [79]. Wang et al. [80] revealed field evidence about the rise in aerosol loading and its link with positive vegetation growth in China.

Interestingly, Chakraborty et al. [81] reported browning over central India, which contradicts the findings of greening in this research: the differences may be due to the approach used in their study. In our study, we tested the trend at different resolutions and with different methods, and in all the results, the greening pattern was dominant (see Figures 12 and 13). Undoubtedly, vegetation greening reveals the presence of sufficient moisture, and the southwest monsoon keeps the landscape free from prolonged water stress. Overall, a browning of vegetation was observed in only a few regions located in MP, the north-west of JH and south of CH and OD. The decreasing rainfall trends over Chhattisgarh are in agreement with ground observation [82].

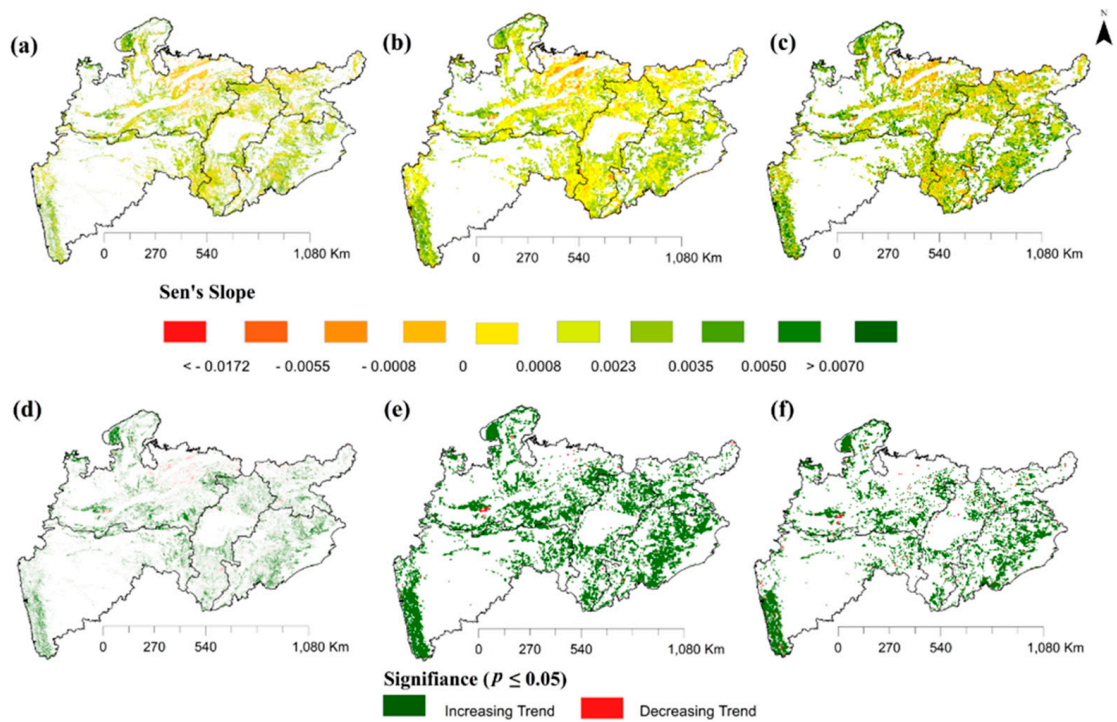


Figure 12. Comparison of (a–c) Sen’s slopes and (d–f) trends from different approaches using annual mean NDVI: (a) based on NDVI_A250, (b) based on NDVI_A5km and (c) based on majority aggregation of reclassified SEN_A250 to 5 km.

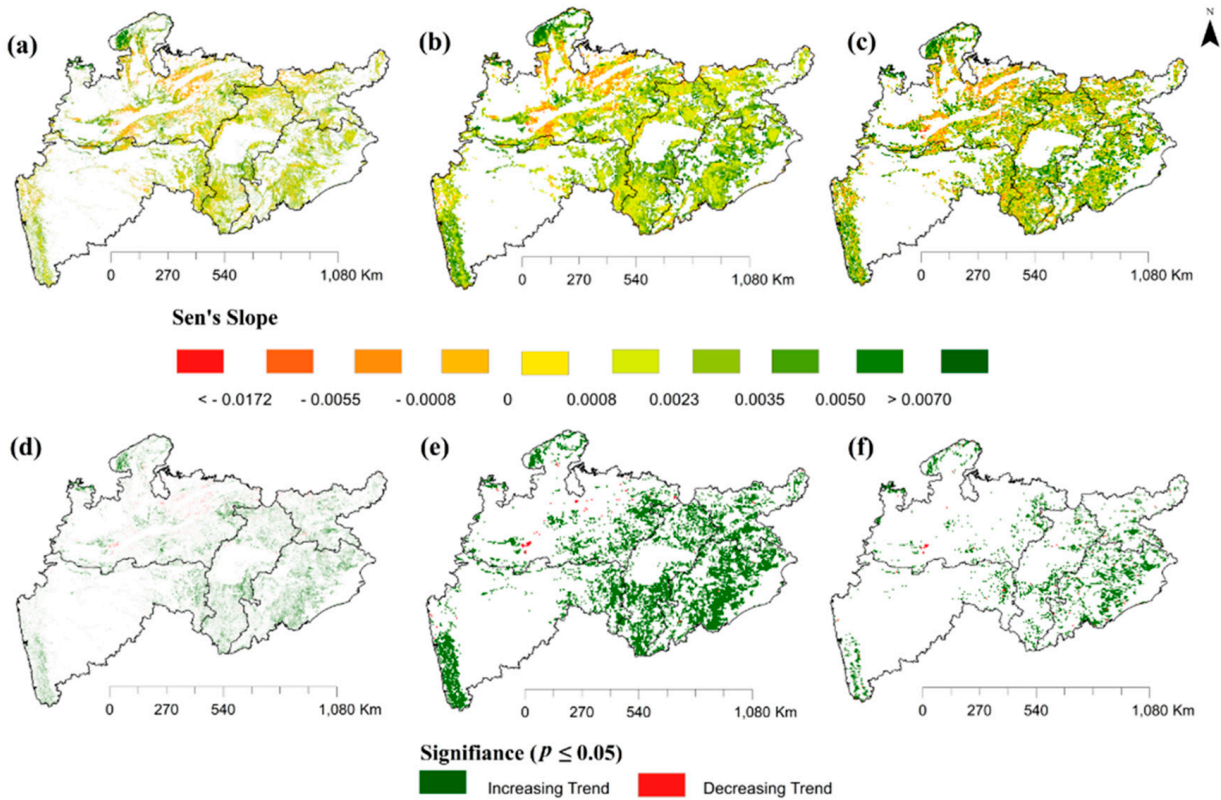


Figure 13. Comparison of (a–c) Sen’s slopes and (d–f) trends from different approaches using mean NDVI from the peak growing period: (a) based on NDVI_P250, (b) based on NDVI_P5 km and (c) based on majority aggregation of reclassified SEN_P250 to 5 km.

The dependency of dry deciduous forest and moist deciduous forest on rainfall varied across the landscape. We observed that the dependency of dry forest on rainfall was much greater than for moist deciduous forest, inferred from the regression analysis using random samples. Several studies reported that the spatial pattern of greening might reveal the water-use capacity of different vegetation types and species in tolerating stress or drought at the regional level [38,83,84]. In our research, the NRR in 2002 was much higher in the drought year than the wet year (i.e., 2013) (Figure 11), which reveals the high resilience of central Indian vegetation, even with low rainfall for a prolonged period [85].

Since the temperature is high throughout the year in central India, water availability increases vegetation photosynthesis; hence, peak growth of vegetation is observed during the monsoon. However, high precipitation does not guarantee high moisture in a region as soil moisture depends on various factors. Here, we assumed that high rainfall positive anomalies in an area are a sign of water availability for vegetation growth and development. However, many factors such as altitude, soil characteristics, root uptake, drainage and runoff, subsurface flow, evapotranspiration and water holding capacity of the soil control water availability in any region [86]. Apparently, in the tropical region, deciduous forest growth is mainly controlled by rainfall. Our results for the spatio-temporal pattern of rainfall and vegetation responses in five-yearly phases showed a divergent response in drier and wetter periods at the regional scale. Ultimately, the undulating terrain of the central Indian landscape plays a vital role in controlling micro-habitat variation and moisture availability due to runoff. In addition, factors such as drought-tolerant species, evapotranspiration, the duration and intensity of rainfall, temperature, elevation gradient and soil types over central India can affect the variability between phases and long-term trends as a whole [87–90].

Samanta et al. [91] observed that warming of the Indian Ocean has a diminishing effect on rainfall in central India, especially during drought years. A significant rise in extreme events was reported over the central Indian landscape with the weakening of the monsoon and increasing spatial variability at local and regional levels [41,92]. As a consequence of climatic change and an imbalance in terrestrial and sea surface warming, central Indian tropical forest ecosystems may experience stress in moisture supply. It results in biodiversity loss, which may affect ecosystem services and life-support systems in the region, impacting the long-term survival of forest-dependent populations.

The effect of upscaling NDVI to 5 km on Sen's slope and the significance of trends was tested. The majority based approach produced a more reliable result as its estimates were close to the estimates using NDVI at a spatial resolution of 250 m (Tables S3 and S4). However, for both NDVI_A5km and NDVI_P5km data, it was observed that Sen's slope classes in the mean-based approach (i.e., SEN_A5km and SEN_P5km) with the small area were underestimated, and Sen's slope classes with the large area were overestimated. Interestingly, the reverse was observed (overestimation of small area classes and vice versa) in the majority-based approach (i.e., SEN'_A5 km and SEN'_P5 km). Although continuous vegetation information can be derived at a very fine spatial resolution up to 20 m, continuous rainfall data at a fine spatial resolution are not yet available. Hence, increasing the spatial resolution of the available rainfall observations needs serious attention from the research community.

5. Conclusions

We used remote sensing-derived vegetation indices and rainfall data over 18 years to investigate the response of central Indian tropical forests to rainfall variation. The research revealed a complex spatial pattern of diverse vegetation responses to rainfall seasonality, expressed through long-term trends and impacts on vegetation in different five-yearly phases. Central Indian vegetation showed resistance to dry spells and water scarcity despite decreasing or deficit rainfall trends. This means that the productivity of vegetation has been sustained even during drought-like conditions in different years. Hence, we

conclude that it has high resilience and water use efficiency relative to climatic oscillations in the region.

Nevertheless, it was found that rainfall impacted vegetation growth to some extent: negatively in a drought year (2002) and positively in a wet year (2013). The research presented here quantified this dependency spatially for the first time. Interestingly, high-density forests in the eastern states of Odisha (OD), Jharkhand (JH) and Chhattisgarh (CH) received a greater amount of rainfall in the summer, providing an interesting focus for further investigation. Greening patterns were observed over 88% of the forested landscape at 250 m spatial resolution, and 2-tier majority-based aggregation of Sen's slope data at 5 km spatial resolution revealed reliable area estimates consistent with those at 250 m.

We recommend that policymakers set up a network of rainfall stations, runoff measurements, phenocams and eddy covariance towers to quantify the impacts of climate change and assess forest vulnerability relative to future changes across central India. Such a network may also help to understand the exchange of carbon and water fluxes, water use efficiency and the impact of droughts at the micro-habitat, watershed, forest type and species levels.

Supplementary Materials: The following figures and tables are available online at <https://www.mdpi.com/article/10.3390/rs13214474/s1>, Figure S1. Spatio-temporal variability of Sen's slope derived from different datasets: (a) based on original CHIRPS and (b) based on Kriging corrected CHIRPS. Figure S2. Validation of significant (a,c) decreasing trends and (b,d) increasing trends. Table S1. Standardised Rainfall Anomaly (SRA) from 2001 to 2018. Table S2. Standardised NDVI Anomaly (SNA) during dry, normal and wet years. Table S3. Area statistics (in %) of Sen's slope derived from different approaches using the Annual Mean NDVI. Table S4. Area statistics (in %) of Sen's slope derived from different approaches using Mean NDVI from the peak-growth period.

Author Contributions: B.S. and C.J. designed the study. B.S., C.J. and V.S.R. participated in data analysis. B.S. created figures with the guidance of C.J., V.S.R., M.D.B., C.P.S., P.S.R. and P.M.A. All the authors wrote and reviewed the manuscript, discussed results and approved the final version. All authors have read and agreed to the published version of the manuscript.

Funding: We acknowledge the support of Birla Institute of Technology, Mesra, Ranchi, which funded the PhD program of BS (Ref. No. OO/Estb/Ph.D/20017-18/2772).

Institutional Review Board Statement: Not Applicable.

Informed Consent Statement: Not Applicable.

Data Availability Statement: Requests for materials should be addressed to BS.

Acknowledgments: The authors thank NASA (Land Processing Distributed Active Archive Centre) for providing the MODIS data and the Climate Hazard Group, University of California Santa Barbara (UCSB), for providing CHIRPS data freely. We also thank all the reviewers for their valuable comments and suggestions which has helped in improving the quality of the manuscript.

Conflicts of Interest: The authors declare no conflict of interest.

References

1. IPCC. *Climate Change 2014: Synthesis Report. Contribution of Working Groups I, II and III to the Fifth Assessment Report of the Intergovernmental Panel on Climate Change*; Pachauri, R.K., Meyer, L.A., Eds.; IPCC: Geneva, Switzerland, 2014; p. 151.
2. Miles, L.; Grainger, A.; Phillips, O. The impact of global climate change on tropical forest biodiversity in Amazonia. *Glob. Ecol. Biogeogr.* **2004**, *13*, 553–565. [[CrossRef](#)]
3. Nobre, C.A.; Obregón, G.O.; Marengo, J.A.; Fu, R.; Poveda, G. Characteristics of Amazonian climate: Main features. In *Amazonia and Global Change*; Keller, M., Bustamante, M., Gash, J., Dias, P.S., Eds.; American Geophysical Union: Washington, DC, USA, 2009.
4. DeFries, R.S.; Rudel, T.; Uriarte, M.; Hansen, M.C. Deforestation driven by urban population growth and agricultural trade in the twenty-first century. *Nat. Geosci.* **2010**, *3*, 178–181. [[CrossRef](#)]
5. Hansen, M.C.; Potapov, P.V.; Moore, R.; Hancher, M.; Turubanova, S.A.; Tyukavina, A.; Thau, D.; Stehman, S.V.; Goetz, S.J.; Loveland, T.R.; et al. High-Resolution Global Maps of 21st-Century Forest Cover Change. *Science* **2013**, *342*, 850–853. [[CrossRef](#)] [[PubMed](#)]

6. FAO. *Global Forest Resources Assessment 2015 How are the World's Forests Changing?* Food and Agriculture Organization of the United Nations Rome: Rome, Italy, 2015; ISBN 978-92-5-109283-5.
7. FAO. *Global Forest Resources Assessment 2020; Main report*; FAO: Rome, Italy, 2020.
8. Muluneh, A.; Van Loon, E.; Bewket, W.; Keesstra, S.; Stroosnijder, L.; Burka, A. Effects of long-term deforestation and remnant forests on rainfall and temperature in the Central Rift Valley of Ethiopia. *For. Ecosyst.* **2017**, *4*. [[CrossRef](#)]
9. Leite-Filho, A.T.; Soares-Filho, B.S.; Davis, J.L.; Abrahão, G.M.; Börner, J. Deforestation reduces rainfall and agricultural revenues in the Brazilian Amazon. *Nat. Commun.* **2021**, *12*, 1–7. [[CrossRef](#)]
10. Houet, T.; Verburg, P.H.; Loveland, T.R. Monitoring and modelling landscape dynamics. *Landsc. Ecol.* **2009**, *25*, 163–167. [[CrossRef](#)]
11. Yang, J.; Weisberg, J.P.; Bristow, A.N. Landsat remote sensing approaches for monitoring long-term tree cover dynamics in semi-arid woodlands, Comparison of vegetation indices and spectral mixture analysis. *Remote Sens. Environ.* **2012**, *119*, 62–71. [[CrossRef](#)]
12. Wulder, M. Optical remote sensing techniques for the assessment of forest inventory and biophysical parameters. *Prog. Phys. Geogr.* **1998**, *22*, 449–476. [[CrossRef](#)]
13. McIver, D.; Wheaton, E. Tomorrow's forests, adapting to a changing climate. *Clim. Change* **2005**, *70*, 273–282. [[CrossRef](#)]
14. Beck, P.S.; Atzberger, C.; Høgda, K.A.; Johansen, B.; Skidmore, A. Improved monitoring of vegetation dynamics at very high latitudes: A new method using MODIS NDVI. *Remote Sens. Environ.* **2006**, *100*, 321–334. [[CrossRef](#)]
15. Körner, C.; Hoch, G. A test of tree line theory on a Montane Permaforest island. *Arct. Antarct. Alp. Res.* **2006**, *38*, 113–119. [[CrossRef](#)]
16. Dong, S.X.; Davies, S.J.; Ashton, P.S.; Bunyavejchewin, S.; Supardi, M.N.N.; Kassim, A.R.; Tan, S.; Moorcroft, P.R. Variability in solar radiation and temperature explains observed patterns and trends in tree growth rates across four tropical forests. *Proc. R. Soc. B Boil. Sci* **2012**, *279*, 3923–3931. [[CrossRef](#)] [[PubMed](#)]
17. Stocker, B.D.; Zscheischler, J.; Keenan, T.F.; Prentice, I.C.; Peñuelas, J.; Seneviratne, S.I. Quantifying soil moisture impacts on light use efficiency across biomes. *New Phytol.* **2018**, *218*, 1430–1449. [[CrossRef](#)]
18. Nemani, R.R.; Keeling, C.D.; Hashimoto, H.; Jolly, W.M.; Piper, S.C.; Tucker, C.J.; Myneni, R.B.; Running, S.W. Climate-Driven Increases in Global Terrestrial Net Primary Production from 1982 to 1999. *Science* **2003**, *300*, 1560–1563. [[CrossRef](#)]
19. Seddon, A.; Macias-Fauria, M.; Long, P.R.; Benz, D.; Willis, K. Sensitivity of global terrestrial ecosystems to climate variability. *Nature* **2016**, *531*, 229–232. [[CrossRef](#)] [[PubMed](#)]
20. Green, J.K.; Berry, J.; Ciais, P.; Zhang, Y.; Gentine, P. Amazon rainforest photosynthesis increases in response to atmospheric dryness. *Sci. Adv.* **2020**, *6*, eabb7232. [[CrossRef](#)]
21. Aubry-Kientz, M.; Rossi, V.; Wagner, F.; Hérault, B. Identifying climatic drivers of tropical forest dynamics. *Biogeosciences* **2015**, *12*, 5583–5596. [[CrossRef](#)]
22. Scranton, K.; Amarasekare, P. Predicting phenological shifts in a changing climate. *Proc. Natl. Acad. Sci. USA* **2017**, *114*, 13212–13217. [[CrossRef](#)]
23. Bohlman, S.A. Landscape patterns and environmental controls of deciduousness in forests of central Panama. *Glob. Ecol. Biogeogr.* **2010**, *19*, 376–385. [[CrossRef](#)]
24. Chaturvedi, R.K.; Raghubanshi, A.S.; Singh, J.S. Plant functional traits with particular reference to tropical deciduous forests: A review. *J. Biosci.* **2011**, *36*, 963–981. [[CrossRef](#)]
25. Li, C.; Qi, J.; Yang, L.; Wang, S.; Yang, W.; Zhu, G.; Zou, S.; Zhang, F. Regional vegetation dynamics and its response to climate change—A case study in the Tao River Basin in Northwestern China. *Environ. Res. Lett.* **2014**, *9*, 125003. [[CrossRef](#)]
26. Paruelo, J.M.; Burke, I.C.; Lauenroth, W.K. Land use impact on ecosystem functioning in eastern Colorado, USA. *Glob. Change Biol.* **2001**, *7*, 631–639.
27. Olsson, L.; Eklundh, L.; Ard, J. A recent greening of the Sahel—Trends, patterns and potential causes. *J. Arid Environ.* **2005**, *63*, 556–566. [[CrossRef](#)]
28. Krishnaswamy, J.; John, R.; Joseph, S. Consistent response of vegetation dynamics to recent climate change in tropical mountain regions. *Glob. Change Biol.* **2013**, *20*, 203–215. [[CrossRef](#)] [[PubMed](#)]
29. Singh, B.; Jeganathan, C.; Rathore, V.S. Improved NDVI based proxy leaf-fall indicator to assess rainfall sensitivity of deciduousness in the central Indian forests through remote sensing. *Sci. Rep.* **2020**, *10*, 17638. [[CrossRef](#)] [[PubMed](#)]
30. Griffin, K.L.; Prager, C.M. Where does the carbon go? Thermal acclimation of respiration and increased photosynthesis in trees at the temperate-boreal ecotone. *Tree Physiol.* **2017**, *37*, 281–284. [[CrossRef](#)]
31. Ravindranath, N.; Sukumar, R. Climate Change and Tropical Forests in India. *Clim. Change* **1998**, *39*, 563–581. [[CrossRef](#)]
32. Polanski, S.; Fallah, B.; Befort, D.J.; Prasad, S.; Cubasch, U. Regional moisture change over India during the past Millennium: A comparison of multi-proxy reconstructions and climate model simulations. *Glob. Planet. Change* **2014**, *122*, 176–185. [[CrossRef](#)]
33. Kumar, P.V.; Naidu, C.V.; Prasanna, K. Inconsistency in the Frequency of Rainfall Events in the Indian Summer Monsoon Season. *Int. J. Climatol.* **2019**, *39*, 4907–4923.
34. Chaturvedi, R.K.; Gopalakrishnan, R.; Jayaraman, M.; Bala, G.; Joshi, N.V.; Sukumar, R.; Ravindranath, N.H. Impact of climate change on Indian forests: A dynamic vegetation modeling approach. *Mitig. Adapt. Strateg. Glob. Change* **2010**, *16*, 119–142. [[CrossRef](#)]

35. Lejeune, Q.; Edouard, L.D.; Benoit, P.G.; Sonia, I.S. Influence of Amazonian deforestation on the future evolution of regional surface fluxes, circulation, surface temperature and precipitation. *Clim. Dyn.* **2015**, *44*, 2769–2786. [[CrossRef](#)]
36. Davidson, E.A.; De Araújo, A.C.; Artaxo, P.; Balch, J.K.; Brown, I.F.; Bustamante, M.; Coe, M.; DeFries, R.S.; Keller, M.; Longo, M.; et al. The Amazon basin in transition. *Nature* **2012**, *481*, 321–328. [[CrossRef](#)]
37. Kumar, V.; Jain, S.K.; Singh, Y. Analysis of long-term rainfall trends in India. *Hydrol. Sci. J.* **2010**, *55*, 484–496. [[CrossRef](#)]
38. Roxy, M.K.; Ritika, K.; Terray, P.; Murtugudde, R.; Ashok, K.; Goswami, B.N. Drying of Indian subcontinent by rapid Indian Ocean warming and a weakening land-sea thermal gradient. *Nat. Commun.* **2015**, *6*, 7423. [[CrossRef](#)] [[PubMed](#)]
39. Goswami, B.N.; Venugopal, V.; Sengupta, D.; Madhusoodanan, M.S.; Xavier, P.K. Increasing Trend of Extreme Rain Events Over India in a Warming Environment. *Science* **2006**, *314*, 1442–1445. [[CrossRef](#)] [[PubMed](#)]
40. Rajeevan, M.; Bhate, J.; Jaswal, A.K. Analysis of variability and trends of extreme rainfall events over India using 104 years of gridded daily rainfall data. *Geophys. Res. Lett.* **2008**, *35*, L18707. [[CrossRef](#)]
41. Roxy, M.K.; Ghosh, S.; Pathak, A.; Athulya, R.; Mujumdar, M.; Murtugudde, R.; Terray, P.; Rajeevan, M. A threefold rise in widespread extreme rain events over central India. *Nat. Commun.* **2017**, *8*, 1–11. [[CrossRef](#)] [[PubMed](#)]
42. Malhi, Y.; Aragão, L.E.O.C.; Galbraith, D.; Huntingford, C.; Fisher, R.; Zelazowski, P.; Sitch, S.; McSweeney, C.; Meir, P. Exploring the likelihood and mechanism of a climate-change induced dieback of the Amazon rainforest. *Proc. Natl Acad. Sci. USA* **2009**, *106*, 20610–20615. [[CrossRef](#)]
43. Cox, P.M.; Pearson, D.; Booth, B.B.; Friedlingstein, P.; Huntingford, C.; Jones, C.D.; Luke, C.M. Sensitivity of tropical carbon to climate change constrained by carbon dioxide variability. *Nature* **2013**, *494*, 341–344. [[CrossRef](#)]
44. Bhargava, S.; Sawant, K. Drought stress adaptation: Metabolic adjustment and regulation of gene expression. *Plant Breed.* **2012**, *132*, 21–32. [[CrossRef](#)]
45. Cristiano, E.; Ten Veldhuis, M.-C.; Van de Giesen, N. Spatial and temporal variability of rainfall and their effects on hydro-logical response in urban areas—A review. *Hydrol. Earth Syst. Sci.* **2017**, *21*, 3859–3878. [[CrossRef](#)]
46. Synodinos, A.D.; Tietjen, B.; Lohmann, D.; Jeltsch, F. The impact of inter-annual rainfall variability on African savannas changes with mean rainfall. *J. Theor. Biol.* **2018**, *437*, 92–100. [[CrossRef](#)] [[PubMed](#)]
47. Conte, A.; Fares, S.; Salvati, L.; Savi, F.; Matteucci, G.; Mazzenga, F.; Spano, D.; Sirca, C.; Marras, S.; Galvagno, M.; et al. Ecophysiological Responses to Rainfall Variability in Grassland and Forests Along a Latitudinal Gradient in Italy. *Front. For. Glob. Change* **2019**, *2*. [[CrossRef](#)]
48. Wang, X.; Ciais, P.; Wang, Y.; Zhu, D. Divergent response of seasonally dry tropical vegetation to climatic variations in dry and wet seasons. *Glob. Change Biol.* **2018**, *24*, 4709–4717. [[CrossRef](#)] [[PubMed](#)]
49. Kulkarni, A.; Gadgil, S.; Patwardhan, S. Monsoon Variability, the 2015 Marathwada Drought and Rainfed Agriculture. *Curr. Sci.* **2016**, *111*. [[CrossRef](#)]
50. Champion, H.G.; Seth, S.K. *A Revised Survey of the Forest Types of India*; Government of India Publication: New Delhi, India, 1968.
51. ISFR. *State of Forest Report Forest Survey of India*; Ministry of Environment and Forests, Government of India: Dehradun, India, 2019.
52. Funk, C.; Peterson, P.; Landsfeld, M.; Pedreros, D.; Verdin, J.; Shukla, S.; Michaelsen, J. The climate hazards infrared precipitation with stations—A new environmental record for monitoring extremes. *Sci. Data.* **2015**, *2*, 150066. [[CrossRef](#)] [[PubMed](#)]
53. Huete, A.; Didan, K.; Miura, T.; Rodriguez, E.; Gao, X.; Ferreira, L. Overview of the radiometric and biophysical performance of the MODIS vegetation indices. *Remote. Sens. Environ.* **2002**, *83*, 195–213. [[CrossRef](#)]
54. Didan, K.; Barreto, A.; Solano, R.; Huete, A. *MODIS Vegetation Index User's Guide (MOD13 Series)*; Version 3.00 (Collection 6); The University of Arizona: Tucson, AZ, USA, 2015.
55. Roy, P.S.; Behera, M.D.; Murthy, M.; Roy, A.; Singh, S.; Kushwaha, S.; Jha, C.; Sudhakar, S.; Joshi, P.; Reddy, S.; et al. New vegetation type map of India prepared using satellite remote sensing: Comparison with global vegetation maps and utilities. *Int. J. Appl. Earth Obs. Geoinformation* **2015**, *39*, 142–159. [[CrossRef](#)]
56. Jeganathan, C.; Dash, J.; Atkinson, P.M. Characterising the spatial pattern of phenology for the tropical vegetation of India using multi-temporal MERIS chlorophyll data. *Landsc. Ecol.* **2010**, *25*, 1125–1141. [[CrossRef](#)]
57. Atkinson, P.M.; Jeganathan, C.; Dash, J.; Atzberger, C. Inter-comparison of four models for smoothing satellite sensor time-series data to estimate vegetation phenology. *Remote. Sens. Environ.* **2012**, *123*, 400–417. [[CrossRef](#)]
58. Pastor-Guzman, J.; Dash, J.; Atkinson, P.M. Remote sensing of mangrove forest phenology and its environmental drivers. *Remote. Sens. Environ.* **2018**, *205*, 71–84. [[CrossRef](#)]
59. Sen, P.K. Estimates of the regression coefficient based on Kendall's tau. *J. Am. Stat. Assoc.* **1968**, *63*, 1379–1389. [[CrossRef](#)]
60. Stow, D.A.; Hope, A.; McGuire, D.; Verbyla, D.; Gamon, J.; Huemmrich, F.; Houston, S.; Racine, C.; Sturm, M.; Tape, K.; et al. Remote sensing of vegetation and land-cover change in Arctic Tundra ecosystems. *Remote Sens. Environ.* **2004**, *89*, 281–308. [[CrossRef](#)]
61. Ahmed, A.; Deb, D.; Mondal, S. Assessment of Rainfall Variability and its Impact on Groundnut Yield in Bundelkhand Region of India. *Curr. Sci.* **2019**, *117*. [[CrossRef](#)]
62. Panda, A.; Sahu, N. Trend analysis of seasonal rainfall and temperature pattern in Kalahandi, Bolangir and Koraput districts of Odisha, India. *Atmos. Sci. Lett.* **2019**, *20*, e932. [[CrossRef](#)]
63. Atkinson, P.M.; Dash, J.; Jeganathan, C. Amazon vegetation greenness as measured by satellite sensors over the last decade. *Geophys. Res. Lett.* **2011**, *38*. [[CrossRef](#)]

64. Qi, H.; Huang, F.; Zhai, H. Monitoring Spatio-Temporal Changes of Terrestrial Ecosystem Soil Water Use Efficiency in Northeast China Using Time Series Remote Sensing Data. *Sensors* **2019**, *19*, 1481. [[CrossRef](#)] [[PubMed](#)]
65. Wang, J.; Rich, P.M.; Price, K.P.; Kettle, W.D. Relations between NDVI and tree productivity in the central Great Plains. *Int. J. Remote. Sens.* **2004**, *25*, 3127–3138. [[CrossRef](#)]
66. Park, T.; Ganguly, S.; Tømmervik, H.; Euskirchen, E.S.; Høgda, K.-A.; Karlsen, S.R.; Brovkin, V.; Nemani, R.R.; Myneni, R. Changes in growing season duration and productivity of northern vegetation inferred from long-term remote sensing data. *Environ. Res. Lett.* **2016**, *11*, 084001. [[CrossRef](#)]
67. Rajan, H.; Jeganathan, C. Understanding Spatio-temporal Pattern of Grassland Phenology in the western Indian Himalayan State. *J. Indian Soc. Remote. Sens.* **2019**, *47*, 1137–1151. [[CrossRef](#)]
68. Shukla, A.N.; Kumar, B.; Srivastava, S.K. Floristic composition and vegetation types of Rewa District in Madhya Pradesh: An overview. *Ann. For.* **2010**, *18*, 283–296.
69. Rathoure, A.K. Ecological status for Ratapani wild life sanctuary, Raisen (MP) India. *Biodivers. Int. J.* **2018**, *2*, 153–170. [[CrossRef](#)]
70. Singh, P.K.; Sahu, S.; Singh, P. Assessment of Richness of Diversity between Various Species of Vegetation Type and Their Threat Status in Mukundpur Forest Area, Satna District, Madhya Pradesh, India. *J. Agric. Ecol. Res. Int.* **2018**, *16*, 1–16. [[CrossRef](#)]
71. Mungi, N.A.; Qureshi, Q.; Jhala, Y.V. Expanding niche and degrading forests: Key to the successful global invasion of *Lantana camara* (sensu lato). *Glob. Ecol. Conserv.* **2020**, *23*, e01080. [[CrossRef](#)]
72. Singh, V.P. *Flora of Madhya Pradesh (Western Part)*; Scientific Publishers: Jodhpur, India, 2014.
73. Paul, S.; Ghosh, S.; Oglesby, R.; Pathak, A.; Chandrasekharan, A.; Ramsankaran, R. Weakening of Indian Summer Monsoon Rainfall due to Changes in Land Use Land Cover. *Sci. Rep.* **2016**, *6*, 32177. [[CrossRef](#)]
74. Putnam, A.E.; Broecker, W.S. Human-induced changes in the distribution of rainfall. *Sci. Adv.* **2017**, *3*, e1600871. [[CrossRef](#)]
75. Rai, P.; Dimri, A.P. Changes in rainfall seasonality pattern over India. *Meteorol. Appl.* **2019**, *27*. [[CrossRef](#)]
76. Reddy, C.S.; Rajashekar, G.; Krishna, P.H.; Jha, C.; Dadhwal, V. Multi-source and multi-date mapping of deforestation in Central India (1935–2010) and its implication on standing phytomass carbon pool. *Ecol. Indic.* **2015**, *57*, 219–227. [[CrossRef](#)]
77. Moorthy, K.K.; Babu, S.S.; Manoj, M.R.; Satheesh, S.K. Buildup of aerosols over the Indian Region. *Geophys. Res. Lett.* **2013**, *40*, 1011–1014. [[CrossRef](#)]
78. Thomas, A.; Sarangi, C.; Kanawade, V.P. Recent Increase in Winter Hazy Days over Central India and the Arabian Sea. *Sci. Rep.* **2019**, *9*, 1–10. [[CrossRef](#)]
79. Sarangi, C.; Tripathi, S.N.; Kanawade, V.P.; Koren, I.; Pai, D.S. Investigation of the aerosol–cloud–rainfall association over the Indian summer monsoon region. *Atmospheric Chem. Phys. Discuss.* **2017**, *17*, 5185–5204. [[CrossRef](#)]
80. Wang, X.; Wu, J.; Chen, M.; Xu, X.; Wang, Z.; Wang, B.; Wang, C.; Piao, S.; Lin, W.; Miao, G.; et al. Field evidences for the positive effects of aerosols on tree growth. *Glob. Chang. Biol.* **2018**, *24*, 4983–4992. [[CrossRef](#)]
81. Chakraborty, A.; Seshasai, M.; Reddy, C.S.; Dadhwal, V. Persistent negative changes in seasonal greenness over different forest types of India using MODIS time series NDVI data (2001–2014). *Ecol. Indic.* **2018**, *85*, 887–903. [[CrossRef](#)]
82. Bhelawe, S.; Chaudhary, J.L.; Nain, A.S.; Singh, R.; Khavse, R.; Chandrawanshi, S.K. Rainfall Variability in Chhattisgarh State Using GIS. *Curr. World Environ.* **2014**, *9*, 519–524. [[CrossRef](#)]
83. Yang, L.; Wylie, B.; Tieszen, L.L.; Reed, B.C. An Analysis of Relationships among Climate Forcing and Time-Integrated NDVI of Grasslands over the U.S. Northern and Central Great Plains. *Remote. Sens. Environ.* **1998**, *65*, 25–37. [[CrossRef](#)]
84. Piao, S.; Fang, J.; Zhou, L.; Guo, Q.; Henderson, M.; Ji, W.; Li, Y.; Tao, S. Interannual variations of monthly and seasonal normalized difference vegetation index (NDVI) in China from 1982 to 1999. *J. Geophys. Res. Space Phys.* **2003**, *108*. [[CrossRef](#)]
85. Huang, L.; He, B.; Han, L.; Liu, J.; Wang, H.; Chen, Z. A global examination of the response of ecosystem water-use efficiency to drought based on MODIS data. *Sci. Total. Environ.* **2017**, *601*, 1097–1107. [[CrossRef](#)]
86. Zeng, C.; Zhang, F.; Wang, Q.; Chen, Y.; Joswiak, D.R. Impact of alpine meadow degradation on soil hydraulic properties over the Qinghai-Tibetan Plateau. *J. Hydrol.* **2012**, *478*, 148–156. [[CrossRef](#)]
87. White, A.B.; Kumar, P.; Tcheng, D. A data mining approach for understanding topographic control on climate-induced interannual vegetation variability over the United States. *Remote Sens. Environ.* **2005**, *98*, 1–20. [[CrossRef](#)]
88. Propastin, P.A.; Kappas, M.; Muratova, N.R. Inter-annual changes in vegetation activities and their relationship to temperature and precipitation in Central Asia from 1982 to 2003. *J. Environ. Inform.* **2008**, *12*, 75–87. [[CrossRef](#)]
89. Jiang, L.; Guli-jiapaer, G.; Bao, A.; Guo, H.; Ndayisaba, F. Vegetation dynamics and responses to climate change and human activities in Central Asia. *Sci. Total Environ.* **2017**, *599*, 967–980. [[CrossRef](#)] [[PubMed](#)]
90. Chen, Z.; Wang, W.; Fu, J. Vegetation response to precipitation anomalies under different climatic and biogeographical conditions in China. *Sci. Rep.* **2020**, *10*, 830. [[CrossRef](#)] [[PubMed](#)]
91. Samanta, D.; Rajagopalan, B.; Karnauskas, K.B.; Zhang, L.; Goodkin, N.F. La Niña’s Diminishing Fingerprint on the Central Indian Summer Monsoon. *Geophys. Res. Lett.* **2020**, *47*, e2019GL086237. [[CrossRef](#)]
92. Ghosh, S.; Vittal, H.; Sharma, T.; Karmakar, S.; Kasiviswanathan, K.S.; Dhanesh, Y.; Sudheer, K.P.; Gunthe, S.S. Indian Summer Monsoon Rainfall: Implications of Contrasting Trends in the Spatial Variability of Means and Extremes. *PLoS ONE* **2016**, *11*, e0158670. [[CrossRef](#)] [[PubMed](#)]